HHS Public Access
Author manuscript
*Cell Rep*. Author manuscript; available in PMC 2023 October 23.

Published in final edited form as:
*Cell Rep*. 2023 February 28; 42(2): 112106. doi:10.1016/j.celrep.2023.112106.

# DRAK2 contributes to type 1 diabetes by negatively regulating IL-2 sensitivity to alter regulatory T cell development

**Alexandra H. Mandarano**[1,4], **Tarsha L. Harris**[1,4], **Blaine M. Creasy**[1], **Marie Wehenkel**[1], **Marygrace Duggar**[1,2], **Benjamin A. Wilander**[1,2], **Ashutosh Mishra**[3], **Jeremy Chase Crawford**[1], **Sarah A. Mullen**[1], **Katherine M. Williams**[1], **Meenu Pillai**[1], **Anthony A. High**[3], **Maureen A. McGargill**[1,5,*]

[1]Department of Immunology, St. Jude Children's Research Hospital, Memphis, TN 38105, USA

[2]St. Jude Graduate School of Biomedical Sciences, Memphis, TN 38105, USA

[3]Center for Proteomics and Metabolomics, St. Jude Children's Research Hospital, Memphis, TN 38105, USA

[4]These authors contributed equally

[5]Lead contact

## SUMMARY

*Drak2*-deficient (*Drak2*$^{-/-}$) mice are resistant to multiple models of autoimmunity yet effectively eliminate pathogens and tumors. Thus, DRAK2 represents a potential target to treat autoimmune diseases. However, the mechanisms by which DRAK2 contributes to autoimmunity, particularly type 1 diabetes (T1D), remain unresolved. Here, we demonstrate that resistance to T1D in non-obese diabetic (*NOD*) mice is due to the absence of *Drak2* in T cells and requires the presence of regulatory T cells ($T_{regs}$). Contrary to previous hypotheses, we show that DRAK2 does not limit TCR signaling. Rather, DRAK2 regulates IL-2 signaling by inhibiting STAT5A phosphorylation. We further demonstrate that enhanced sensitivity to IL-2 in the absence of Drak2 augments thymic $T_{reg}$ development. Overall, our data indicate that DRAK2 contributes to autoimmunity in multiple ways by regulating thymic $T_{reg}$ development and by impacting the sensitivity of conventional T cells to $T_{reg}$-mediated suppression.

## Graphical Abstract



*Correspondence: maureen.mcgargill@stjude.org.

AUTHOR CONTRIBUTIONS

A.H.M., T.L.H., B.M.C., A.M., and M.A.M. designed the experiments. All authors conducted experiments and analyzed data. A.H.M. and M.A.M. wrote the manuscript. M.W., M.A.M., A.H.M., T.L.H., M.D., B.A.W., A.M., and J.C.C. revised the manuscript. All authors approved of the final paper.

DECLARATION OF INTERESTS

The authors declare no competing interests.

SUPPLEMENTAL INFORMATION

Supplemental information can be found online at https://doi.org/10.1016/j.celrep.2023.112106.

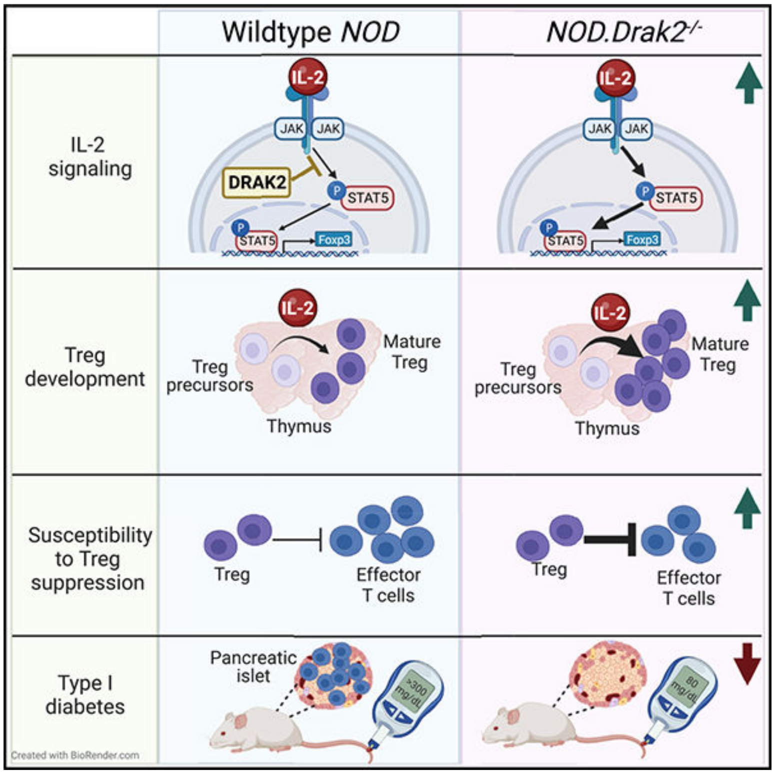


## In brief

DRAK2 represents a potential target to treat autoimmunity without compromising immunity to pathogens. Mandarano et al. show that DRAK2 contributes to autoimmunity by limiting IL-2 signaling, which impacts $T_{reg}$ development. In addition, DRAK2 influences susceptibility of conventional T cells to $T_{reg}$-mediated suppression. These data provide insight for improving treatment of autoimmunity.

## INTRODUCTION

An estimated 23.5 million Americans suffer from autoimmune diseases, and the incidence of these diseases, including type 1 diabetes (T1D), is rising worldwide.[1–7] T1D is caused by autoimmune destruction of pancreatic β-islet cells, which synthesize insulin to control glucose levels in the body.[8] Although glucose homeostasis in T1D is achieved through daily insulin injections, this treatment is not curative and does not prevent other co-morbidities.[5,6] While successful methods have been developed to replace β-islet cells through transplantation or regenerative therapies, the islet cells remain susceptible to attack by autoreactive T cells.[8,9] Thus, an effective cure for T1D would require pancreatic islet cell replacement, as well as inhibition of autoreactive T cells, while sparing pathogen- and tumor-specific T cells.

DRAK2 (also called Stk17b) is a serine/threonine kinase highly expressed in T and B lymphocytes.[10,11] *Drak2*$^{-/-}$ mice are resistant to disease in the experimental autoimmune encephalomyelitis (EAE) model of multiple sclerosis, and the non-obese diabetic (NOD) model of T1D.[11,12] Resistance to disease in these models is partly due to a lack of *Drak2*$^{-/-}$ T cell accumulation in the central nervous system or the pancreas. However, *Drak2*$^{-/-}$ mice mount an effective immune response against multiple pathogens and tumors.[12–15] Thus, targeting DRAK2 is a potential avenue to specifically suppress autoreactive T cells without compromising immunity to infection or tumors.

While previous work demonstrated that DRAK2 induces apoptosis, phosphorylates p70S6K, regulates mitochondrial function, and inhibits TGF-β signaling, it is not clear whether DRAK2 mediates these functions in T cells.[10,16–20] For example, although DRAK2 inhibited TGF-β signaling in cell lines, we demonstrated that DRAK2 did not regulate TGF-β signaling in T cells.[21] Moreover, cell lines lacking *Drak2* exhibited apoptosis defects, but *Drak2*$^{-/-}$ T cells were more sensitive to apoptosis compared with wild-type T cells.[12,22] In naive T cells, *Drak2* is expressed at high levels. Following stimulation, DRAK2 is autophosphorylated in a calcium-dependent manner, and levels of *Drak2* mRNA decrease within 24 h.[11,16,23,24] DRAK2 inhibits calcium signaling and T cell activation, as demonstrated by increased calcium flux and hypersensitivity to suboptimal stimulation in *Drak2*$^{-/-}$ T cells relative to wild-type T cells.[11,24–26] Although DRAK2 regulates T cell activation, the precise mechanisms through which this occurs are unclear. Moreover, how DRAK2 impacts autoimmune disease remains unresolved. We previously demonstrated that EAE resistance resulted from the absence of *Drak2* in T cells.[12] However, it is not known whether *Drak2* within T cells contributes to T1D, as *Drak2* expression is induced in pancreatic β cells after stimulation with free fatty acids or cytokines. In addition, transgenic expression of *Drak2* in β-islet cells enhances β-islet cell apoptosis and renders mice more sensitive to streptozotocin-induced diabetes.[17,27] Thus, *Drak2* expression in islet cells may contribute to T1D pathogenesis.

Here, we investigated whether the absence of *Drak2* in T cells, β-islet cells, or both cell types contributed to T1D resistance. We found that resistance to T1D in *NOD.Drak2*$^{-/-}$ mice was due to *Drak2* deficiency in T cells, and that absence of *Drak2* in pancreatic β cells did not alter T1D incidence. In addition, we show that DRAK2 impacts T1D development through multiple mechanisms affecting both regulatory T cells ($T_{reg}$) and conventional T cells. Unexpectedly, we found that DRAK2 regulates IL-2 signaling by blocking STAT5A phosphorylation. Consequently, *Drak2*$^{-/-}$ mice exhibited enhanced $T_{reg}$ development due to increased IL-2 signaling compared with wild-type mice. Our results reveal previously unknown regulatory functions for DRAK2 within T cells that contribute to autoimmune disease.

## RESULTS

### The resistance to T1D in *NOD.Drak2*$^{-/-}$ mice is dependent on *Drak2* expression in T cells

*NOD* mice, which spontaneously develop T1D, are remarkably resistant to disease in the absence of *Drak2*.[12] To determine whether DRAK2 contributes to T1D by functioning in T cells or other cell types, we performed T cell transfer experiments with NOD mice. We transferred purified CD4$^{+}$ and CD8$^{+}$ T cells from *NOD* or *NOD.Drak2*$^{-/-}$ mice into *NOD.SCID* hosts, which lack T cells but have normal *Drak2* expression in all other cells, including β-islet cells. We monitored mice weekly for development of diabetes via blood glucose levels. Mice that received *NOD.Drak2*$^{-/-}$ T cells were resistant to disease, despite normal expression of *Drak2* in β-islet cells (Figure 1A), while all mice that received wild-type T cells developed T1D by age 20 weeks. Mice that received *NOD* or *NOD.Drak2*$^{-/-}$ T cells had similar numbers of transferred T cells in the blood 11 weeks after transfer (Figure 1B). These data indicate that, although mice receiving *Drak2*$^{-/-}$ T cells did not develop T1D, the *Drak2*$^{-/-}$ T cells were present at the time when wild-type T cells induced T1D. Notably, the proportions of $CD4^+$ and $CD8^+$ T cells were similar in mice that received NOD or *NOD.Drak2*$^{-/-}$ T cells. Overall, the absence of *Drak2* in T cells was sufficient to transfer resistance to T1D.

To further explore whether *Drak2* expression in β-islet cells contributes to disease development, we performed additional cell transfer experiments with *Drak2* expression in T cells, but not β-islet cells or other cell types. Wild-type *NOD* T cells were transferred into *NOD.SCID* or *NOD.Drak2*$^{-/-}$*.SCID* host mice. Both *NOD.SCID* and *NOD.Drak2*$^{-/-}$.SCID mice receiving wild-type T cells developed T1D to a similar extent, despite the absence of *Drak2* in β-islet cells of *NOD.Drak2*$^{-/-}$*.SCID* mice (Figure 1C). *NOD.SCID* and *NOD.Drak2*$^{-/-}$*.SCID* mice had comparable numbers of transferred T cells and proportions of $CD4^+$ and $CD8^+$ T cells in the blood 7 weeks after transfer (Figure 1D). These results reveal that lack of *Drak2* expression in islets is not sufficient to protect against T1D. Moreover, expression of *Drak2* in T cells, rather than b-islet cells, influences T1D susceptibility.

### The resistance to T1D in *NOD.Drak2*$^{-/-}$ mice requires $T_{regs}$

We next investigated whether *Drak2* contributes to T1D by functioning in conventional T cells, $T_{regs}$, or both. Since transferring effector T cells without $T_{regs}$ into lymphopenic hosts can induce colitis and other autoimmune symptoms before diabetes onset, we used *BDC2.5* T cell receptor (TCR) transgenic T cells for these experiments. *BDC2.5* T cells are $CD4^+$ T cells that express a TCR specific for an islet autoantigen, which allowed us to dissect the role of *Drak2* in conventional T cells and $T_{regs}$ during T1D development. We purified and transferred naive, conventional T cells from *BDC2.5* or *Drak2*$^{-/-}$*.BDC2.5* mice into *NOD.SCID* host mice with increasing numbers of wild-type, polyclonal *NOD* $T_{regs}$ (Figure 2A). In the absence of $T_{regs}$, all mice that received *BDC2.5* T cells developed T1D regardless of *Drak2* expression (Figure 2B). The onset of T1D was slightly delayed in mice that received *Drak2*$^{-/-}$ T cells compared with wild-type T cells, but this difference was not significant, indicating that, although *Drak2*$^{-/-}$ T cells are more susceptible to apoptosis than wild-type T cells,[12,22] lack of *Drak2* expression in conventional T cells is not sufficient to confer disease resistance. However, in the presence of wild-type $T_{regs}$, mice that received *Drak2*$^{-/-}$*.BDC2.5* T cells had significantly lower disease incidence than those that received *BDC2.5* T cells (Figures 2C and 2D), which was especially evident by comparing the area under the curve of diabetes incidence induced by wild-type vs. *Drak2*$^{-/-}$ *BDC2.5* T cells (Figure 2F). The numbers of transferred $T_{regs}$ and conventional T cells (Figures 2G and 2H) in the blood, as well as the proportion of $CD4^+$ cells that were $Foxp3^+$ after transfer (Figure 2I), were similar between mice given wild-type or *Drak2*$^{-/-}$ *BDC2.5* conventional T cells. Thus, the presence of wild-type $T_{regs}$ restored the resistance to T1D conferred by *Drak2*$^{-/-}$ T cells. Furthermore, mice that received *Drak2*$^{-/-}$*.BDC2.5* T cells were better protected with fewer wild-type $T_{regs}$ than mice that received *BDC2.5* T cells (Figures 2C–2F), suggesting that *Drak2*$^{-/-}$ conventional T cells are more susceptible to $T_{reg}$ suppression than wild-type T cells. The increased susceptibility to $T_{reg}$ suppression observed for *Drak2*$^{-/-}$ T cells may be related to the previously described enhanced sensitivity to apoptosis compared with wild-type T cells.[12,22] These data indicate that *Drak2* expression within conventional T cells contributes to T1D, but that, in the absence of $T_{regs}$, DRAK2 is not required to induce T1D. These findings are consistent with previous data demonstrating that *Drak2*$^{-/-}$Tcells cause disease in the absence of $T_{regs}$ in the lymphopenia-induced colitis model.[12]

## *Drak2*-deficient $T_{regs}$ function comparably with wild-type $T_{regs}$

As $T_{regs}$ were required for T1D resistance in transfer experiments with *NOD.Drak2*$^{-/-}$ T cells, we examined *NOD.Drak2*$^{-/-}$ $T_{reg}$ function. We stimulated wild-type T cells in vitro, either alone, or with varying ratios of wild-type or *Drak2*$^{-/-}$ $T_{regs}$, for 72 h. As expected, the number of live, divided, conventional T cells decreased with increasing amounts of $T_{regs}$ (Figures S1A and S1B). However, wild-type and *Drak2*$^{-/-}$ $T_{regs}$ suppressed conventional T cell proliferation to a similar extent *in vitro* (Figures S1A and S1B). To test $T_{reg}$ suppression *in vivo*, we transferred naive, *NOD* T cells into *NOD.SCID* mice and evaluated the ability of *NOD* or *NOD.Drak2*$^{-/-}$ $T_{regs}$ to inhibit homeostatic proliferation of wild-type conventional T cells. The proportion of live, divided, conventional T cells was reduced with the addition of $T_{regs}$ (Figure S1C). Yet, the ability of wild-type and *Drak2*$^{-/-}$ $T_{regs}$ to suppress conventional T cell proliferation still did not differ (Figure S1C).

To further assess whether DRAK2 impacts $T_{reg}$ function, we performed microarray analysis on $T_{regs}$ purified from lymph nodes of *NOD* or *NOD.Drak2*$^{-/-}$ mice. Overall gene expression patterns were not significantly different between *NOD* and *NOD.Drak2*$^{-/-}$ $T_{regs}$ (Figures S2A and S2B). Of 20,000 genes analyzed, only 1 gene, Islr, was differentially expressed between *NOD* and *NOD.Drak2*$^{-/-}$ $T_{regs}$ (Figure S2B). In addition, flow cytometry analysis of peripheral $T_{regs}$ revealed no phenotypic differences between *NOD* and *NOD.Drak2*$^{-/-}$ $T_{regs}$ based on expression of several markers (Figures S2C–S2E). Furthermore, the proportion of $T_{regs}$ in the pancreas that were $CD25^{+}$, and the level of CD25 expression on pancreatic $T_{regs}$, were similar between *NOD* and *NOD.Drak2*$^{-/-}$ mice (Figures S2F–S2G). Thus, *Drak2*$^{-/-}$ $T_{regs}$ function similarly to wild-type $T_{regs,}$ and DRAK2 does not significantly impact the phenotype or suppressive function of $T_{regs.}$ Furthermore, T1D resistance in *NOD.Drak2*$^{-/-}$ mice is not due to an augmented ability of *Drak2*$^{-/-}$ $T_{regs}$ to suppress effector T cells.

## DRAK2 alters the abundance of $T_{regs}$s

Since $T_{regs}$ were required for disease resistance in *NOD.Drak2*$^{-/-}$ mice and the abundance of $T_{regs}$ significantly impacted T1D incidence in T cell transfer experiments (Figure 2), we investigated whether the proportion and number of peripheral $T_{regs}$ differed between *NOD* and *NOD.Drak2*$^{-/-}$ mice. At age 13 weeks, a greater proportion of $CD4^{+}$ T cells in the spleen, lymph nodes, and pancreas were $Foxp3^{+}$ in *NOD.Drak2*$^{-/-}$ mice compared with *NOD* mice (Figure 3A). Moreover, the absolute number of $T_{regs}$ in lymph nodes of *NOD.Drak2*$^{-/-}$ mice was higher than NOD mice. While the number of $T_{regs}$ in the pancreas of *NOD.Drak2*$^{-/-}$ mice trended higher, due to variability in overall lymphocyte numbers, the difference was not significant. Nevertheless, these data indicate that a greater proportion of $CD4^+$ T cells are $T_{regs}$ in *NOD.Drak2*$^{-/-}$ vs. *NOD* mice. The increase in $T_{reg}$ number was accompanied by a decrease in the number of conventional $CD4^+$ and $CD8^+$ T cells in the spleen, but not the lymph nodes or pancreas (Figures S3A and S3B).

Since onset of insulitis typically occurs in *NOD* mice at age 6 weeks and could impact $T_{reg}$ frequency, we also examined the spleen and lymph nodes in mice at age 4 weeks. Similar to older mice, we found a significant increase in the number of $T_{regs}$ in the spleen and lymph nodes of *NOD.Drak2*$^{-/-}$ mice compared with *NOD* mice at age 4 weeks (Figure 3B). Moreover, the proportion of $CD4^+$ cells in the spleen that were $Foxp3^+$ was higher in *NOD.Drak2*$^{-/-}$ mice compared with *NOD* mice (Figure 3B). At age 4 weeks, *NOD.Drak2*$^{-/-}$ mice had a reduction in the proportion of conventional $CD4^+$ and $CD8^+$ T cells in the spleen, but an increase in the number of $CD4^+$ conventional T cells in the lymph nodes compared with *NOD* mice (Figure S3C). These data suggest that DRAK2 influences T1D incidence not only by impacting the susceptibility of conventional T cells to $T_{reg}$-mediated suppression but also by altering $T_{reg}$ prevalence.

To determine whether the impact of DRAK2 on $T_{reg}$ abundance was specific to *NOD* mice, we also analyzed $T_{regs}$ in *C57BL/6* and *C57BL/6.*Drak2$^{-/-}$ mice. Similar to the *NOD* mice, there was a significant increase in the $T_{reg}$ proportion in the spleen and lymph nodes of 13-week-old *C57BL/6.Drak2*$^{-/-}$ mice compared with *C57BL/6* mice (Figure 3C). In addition, the number of $T_{regs}$ in lymph nodes of *C57BL/6.Drak2*$^{-/-}$ mice was higher, while the number of conventional T cells in the spleen was reduced compared with *C57BL/6* mice (Figure S3D). Thus, DRAK2 negatively regulates $T_{reg}$ abundance, regardless of mouse strain. Furthermore, the number of conventional T cells is reduced in the spleen, but not lymph nodes or pancreas of *Drak2*$^{-/-}$ mice.

### *Drak2* expression does not impact the induction of peripheral $T_{regs}$

Increased $T_{regs}$ in *Drak2*$^{-/-}$ mice could result from enhanced development of $T_{regs}$ in the thymus or increased peripheral induction of $T_{regs}$. To determine whether Drak2 impacted peripheral $T_{reg}$ induction, we used *OT-II* TCR transgenic mice, in which T cells express a TCR specific for an ovalbumin peptide (I-$A^b$/$OVA_{323–339}$). We first assayed $T_{reg}$ induction in vitro, by stimulating *OT-II* and *OT-II.Drak2*$^{-/-}$ naive T cells with irradiated, $OVA_{323–339}$ peptide-pulsed splenocytes and increasing concentrations of TGF-β for 3 days. We observed a similar induction of $CD4^+Foxp3^+$ $T_{regs}$ among wild-type and *Drak2*$^{-/-}$ T cells as TGF-β concentration increased (Figure S4A). Interestingly, $T_{reg}$ induction among *Drak2*$^{-/-}$ T cells cultured with TGF-β was slightly, but significantly reduced compared with wild-type T cells (Figure S4A), which is contrary to enhanced induction of peripheral $T_{regs}$. To examine $T_{reg}$ induction in vivo, we transferred naive *OT-II* and *OT-II.Drak2*$^{-/-}$ T cells, mixed at a 1:1 ratio, into congenically marked wild-type mice that were given water with or without 2% ovalbumin for 5 days, to elicit induction of $T_{regs}$. The percent and number of induced $Foxp3^+CD4^+$ $T_{regs}$ was comparable between *OT-II* and *OT-II.Drak2*$^{-/-}$ cells, again indicating that induction of $T_{regs}$ was not enhanced in the absence of *Drak2* (Figure S4B). In fact, there was a significantly lower percentage, but not number, of *Drak2*$^{-/-}$ $T_{regs}$ compared with wild-type $T_{regs}$ in mesenteric lymph nodes from mice treated with 2%

ovalbumin (Figure S4B). Together, these data demonstrate that DRAK2 does not regulate peripheral $T_{reg}$ induction. Thus, the increased proportion of $T_{regs}$ in *Drak2*$^{-/-}$ mice is not a consequence of enhanced peripheral $T_{reg}$ induction.

## *Drak2*$^{-/-}$ mice exhibit enhanced $T_{reg}$ development in the thymus compared with wild-type mice

Since *Drak2*$^{-/-}$ mice have a higher proportion of peripheral $T_{regs}$ as early as age 4 weeks, yet do not exhibit enhanced peripheral $T_{reg}$ induction, we examined whether DRAK2 impacted thymic $T_{reg}$ development. $T_{regs}$ develop in the thymus in a two-step process that first involves TCR signaling, which gives rise to two $T_{reg}$ precursor populations: $CD25^+$ precursor $T_{regs}$ ($Foxp3^{neg}CD25^+$) and $Foxp3^{lo}$ precursor $T_{regs}$ ($CD25^{neg}Foxp3^{lo}$).[28,29] In the second step of development, IL-2 signaling mediates the transition of $T_{reg}$ precursors to mature $T_{regs}$ ($CD25^+Foxp3^+$). Thus, we compared the number and proportion of precursor and mature $T_{regs}$ among $CD4^+CD8$ (CD4 SP) thymocytes from *NOD* and *NOD.Drak2*$^{-/-}$ mice at age 4 weeks. *NOD.Drak2*$^{-/-}$ thymii had a significantly higher frequency and number of mature $T_{regs}$ compared with *NOD* thymii (Figure 4A). Interestingly, *NOD.Drak2*$^{-/-}$ mice had a slightly reduced proportion, but not number, of $CD25^+$ precursor $T_{regs}$ (Figure 4A). Since the number of $CD25^+$ precursors was similar between NOD and *NOD.Drak2*$^{-/-}$ mice, yet mature $T_{regs}$ were significantly increased, DRAK2 may impact the transition from $CD25^+$ precursor $T_{reg}$ to mature $T_{reg}$. However, *NOD.Drak2*$^{-/-}$ mice also had a small increase in the proportion and number of $Foxp3^{lo}$ precursor $T_{regs}$ compared with *NOD* mice, which could contribute to the increase in mature $T_{regs}$ (Figure 4A).

As peripheral inflammation could impact thymic development, we next examined whether DRAK2 affects $T_{reg}$ development in neonates, prior to potential influence from the periphery. To obtain sufficient numbers of mice in the same litter, we compared thymii of 1-day-old *NOD.Drak2*$^{+/-}$ and *NOD.Drak2*$^{-/-}$ mice. Just 1 day after birth, *NOD.Drak2*$^{-/-}$ mice had significantly higher proportions and numbers of mature $T_{regs}$ and $Foxp3^{lo}$ precursor $T_{regs}$ compared with *NOD.Drak2*$^{+/-}$ mice, similar to thymii from 4-week-old mice (Figure 4B). As development of both mature $T_{regs}$ and $Foxp3^{lo}$ precursor $T_{regs}$ involves induction of *Foxp3* expression, these data suggest that DRAK2 may negatively regulate induction of *Foxp3* during thymic development.

To determine whether DRAK2 influenced $T_{reg}$ development in mice that are not prone to T1D, we analyzed thymii from *C57BL/6* and *C57BL/6.Drak2*$^{-/-}$ mice at age 4 weeks. Similar to *NOD. Drak2*$^{-/-}$ mice, *C57BL/6. Drak2*$^{-/-}$ mice had a significantly higher proportion and number of mature $T_{regs}$ and no differences in the abundance of $CD25^+$ $T_{reg}$ precursors compared with wild-type mice (Figure 4C). Together, these data demonstrate that DRAK2 impacts mature $T_{reg}$ abundance during thymic development. Thus, the increase in peripheral $T_{regs}$ in *Drak2*$^{-/-}$ mice was due to enhanced thymic development, rather than peripheral induction.

## *Drak2* does not impact TCR signaling in developing thymocytes or mature T cells

The first step of $T_{reg}$ development requires TCR signaling. The strength of the TCR signal impacts cell fate, with higher avidity TCR signals favoring $T_{reg}$ development over conventional T cells.[30] As *Drak2*$^{-/-}$ T cells are hypersensitive to suboptimal TCR stimulation,[11] we investigated whether the absence of *Drak2* augmented $T_{reg}$ development by increasing TCR signaling. *Nur77*$^{GFP}$ reporter mice express GFP following TCR signaling, and GFP expression correlates with TCR signal strength.[31,32] We compared Nur77-GFP mean fluorescence intensity (MFI) throughout thymocyte development in *Nur77*$^{GFP}$ or *Drak2*$^{-/-}$.*Nur77*$^{GFP}$ mice at age 4–6 weeks. In thymii, the $CD4^{-}CD8^{-}$ double-negative (DN) population consists of Nur77-$GFP^{lo}$ and Nur77-$GFP^{int}$ populations, indicating thymocytes before and after TCRβ selection (Figure 5A). During the $CD4^{+}CD8^{+}$ double-positive (DP) stage, high levels of CD69 denote thymocytes that recently underwent positive selection following TCR signaling. Accordingly, we observed a substantial increase in Nur77-GFP expression from $CD69^{lo}$ to $CD69^{hi}$ DP thymocytes (Figures 5A and 5B). Importantly, wild-type and *Drak2*$^{-/-}$ thymocytes had similar Nur77-GFP MFI from the DN stage through the $CD69^{hi}$ DP stage following positive selection, indicating that TCR signal strength is not amplified in the absence of *Drak2* during TCRβ selection and positive selection (Figures 5A and 5B). To specifically examine whether DRAK2 impacts TCR signal strength in developing $T_{regs}$, we analyzed Nur77-GFP MFI in precursor and mature $T_{regs}$. As expected, Nur77-GFP MFI was significantly higher in precursor and mature $T_{reg}$ populations relative to other thymic subsets, reflecting the high avidity TCR signals that drive development of these cells (Figures 5A and 5B). However, Nur77-GFP MFI did not differ between wild-type and *Drak2*$^{-/-}$ thymocytes at either the precursor or mature $T_{reg}$ stage (Figures 5A and 5B). These data demonstrate that *Drak2* expression does not alter TCR signal strength in developing thymocytes.

Since we previously found that *Drak2*$^{-/-}$ T cells were hypersensitive to suboptimal TCR stimulation,[11] we next investigated whether DRAK2 regulates TCR signaling in peripheral T cells. We stimulated $CD8^{+}$ T cells from *OT-I.Nur77*$^{GFP}$ or *OT-I. Drak2*$^{-/-}$.*Nur77*$^{GFP}$ mice with irradiated antigen-presenting cells pulsed with increasing concentrations of either high-affinity ovalbumin peptide ($OVA_{257–264}$) or an altered peptide ligand (OVA-G4), which binds the OT-I TCR with lower affinity than $OVA_{257–264}$. Unexpectedly, Nur77-GFP MFI was not elevated in *Drak2*$^{-/-}$ $CD8^{+}$ T cells stimulated with either low- or high-affinity peptide compared with wild-type $CD8^{+}$ T cells (Figure 5C). Instead, Nur77-GFP was significantly decreased in *Drak2*$^{-/-}$ $CD8^{+}$ T cells stimulated with higher concentrations of both low-and high-affinity peptide compared with $CD8^{+}$ wild-type T cells (Figure 5C). Thus, although OT-I. *Drak2*$^{-/-}$ T cells proliferate more in response to OVA-G4 peptide compared with *OT-I T* cells,[11] these data demonstrate that *Drak2*$^{-/-}$ T cell hyperproliferation is not due to increased TCR signaling. Together, these data indicate that DRAK2 does not negatively regulate TCR signal strength in either developing or mature T cells, suggesting that augmented $T_{reg}$ development in *Drak2*$^{-/-}$ mice is not due to enhanced TCR signal strength. Rather, DRAK2 may regulate T cell activation by modulating signaling pathways distinct from the TCR signaling cascade.

### DRAK2 negatively regulates IL-2 signaling in *NOD* thymocytes

After TCR engagement, the transition from precursor to mature $T_{reg}$ is mediated by IL-2.[33] As DRAK2 did not impact TCR signal strength, we examined whether DRAK2 influenced $T_{reg}$ development by regulating IL-2 signaling. We cultured *NOD* and *NOD. Drak2*$^{-/-}$

thymocytes in medium with or without IL-2 and analyzed phosphorylation of STAT5A Y694 (pSTAT5) via flow cytometry. STAT5A is a transcription factor required for IL-2-mediated induction of *Foxp3* in developing $T_{regs}$ and is activated by JAK-mediated phosphorylation at Y694.[29,34] As expected, pSTAT5A was not detected in the absence of IL-2 but was induced in all $T_{reg}$ populations cultured with IL-2 (Figures 6A–6D). Interestingly, STAT5A phosphorylation was significantly increased in precursor $T_{regs}$ from *NOD. Drak2*$^{-/-}$ mice compared with *NOD* mice (Figures 6A–6C). To determine whether DRAK2 regulates STAT5A phosphorylation in response to other cytokines, thymocytes were also cultured with IL-4, IL-7, or IL-15. In all $T_{reg}$ populations, STAT5A phosphorylation was not increased in *NOD. Drak2*$^{-/-}$ thymocytes cultured with IL-4, IL-7, and IL-15 compared with *NOD* thymocytes (Figure S5A). Rather, there was a small reduction in IL-4-induced pSTAT5A in *NOD. Drak2*$^{-/-}$ Foxp3$^{lo}$ precursor $T_{regs}$ compared with *NOD* Foxp3$^{lo}$ precursor $T_{regs}$ (Figure S5A). These findings demonstrate an increased sensitivity to IL-2 signaling in $T_{reg}$ precursors lacking *Drak2*, suggesting that DRAK2 negatively regulates IL-2 signaling in $T_{reg}$ precursors.

Since IL-2 signaling in thymocytes was enhanced in the absence of *Drak2*, we also investigated whether IL-2 sensitivity was increased in peripheral T cells. We cultured T cells isolated from lymph nodes of *NOD* and *NOD. Drak2*$^{-/-}$ mice with increasing concentrations of IL-2 and evaluated STAT5A phosphorylation in conventional T cells and $T_{regs}$. IL-2 induced slightly increased STAT5A phosphorylation in *NOD. Drak2*$^{-/-}$ peripheral $T_{regs}$ compared with *NOD* $T_{regs}$ (Figure 6E). However, there was no difference in STAT5 phosphorylation between *NOD* and *NOD. Drak2*$^{-/-}$ conventional CD4$^{+}$ or CD8$^{+}$ T cells following IL-2 stimulation (Figures S5B and S5C). Thus, DRAK2 appears to regulate IL-2 signaling primarily in developing thymocytes.

The IL-2 receptor consists of a heterodimer of IL-2Rβ (CD122) and IL-2Rγ (CD132) or a heterotrimer of CD122, CD132, and IL-2Rα (CD25), which binds IL-2 with high affinity.[35] As *Drak2*$^{-/-}$ thymocytes exhibited increased pSTAT5A in response to IL-2, we examined whether expression of the IL-2 receptor chains was similar between wild-type and *Drak2*$^{-/-}$ thymocytes. We found no difference in the level of CD25 on thymic precursor or mature $T_{regs}$ from *NOD. Drak2*$^{-/-}$ and *NOD* mice (Figure 6F). Unexpectedly, expression of CD122 and CD132 was lower on Foxp3$^{lo}$ $T_{reg}$ precursors and CD122 expression was reduced on mature $T_{regs}$ from *Drak2*$^{-/-}$ mice compared with wild-type mice (Figure 6F). These data indicate that sensitivity to IL-2 signaling in *Drak2*$^{-/-}$ thymocytes does not result from increased expression of IL-2 receptor proteins. Rather, DRAK2 impacts IL-2 signaling downstream of the receptors.

To test whether enhanced sensitivity to IL-2 in *Drak2*$^{-/-}$ thymocytes leads to augmented $T_{reg}$ development, we cultured thymocytes from 1-day-old *NOD.Drak2*$^{+/-}$ and *NOD. Drak2*$^{-/-}$ mice *in vitro* with increasing concentrations of IL-2 and evaluated the number of Foxp3$^{+}$ cells the following day. We found that the number and proportion of Foxp3$^{+}$ T cells was significantly higher among *NOD. Drak2*$^{-/-}$ thymocytes compared with *NOD.Drak2*$^{+/}$ thymocytes following IL-2 stimulation (Figure 6G). Thus, *Drak2*$^{-/-}$ thymocytes are more sensitive to IL-2 signaling, and this signaling directly enhances development of mature thymic $T_{regs}$.

To determine whether the absence of *Drak2* impacted IL-2 sensitivity and enhanced thymic $T_{reg}$ development *in vivo*, we injected IL-2/anti-IL-2 complexes into *NOD. Drak2*$^{-/-}$ and *NOD* mice daily for 3 days.[36] Two days after the final injection, we examined $T_{reg}$ abundance in thymii and lymph nodes. As expected, *NOD. Drak2*$^{-/-}$ mice that did not receive IL-2/anti-IL2 complexes had more $T_{regs}$ in both the thymus (Figure 6H) and lymph nodes (Figure S5D) compared with *NOD* mice. While IL-2/anti-IL2 complexes increased the number of $T_{regs}$ in the thymus and lymph nodes of both *NOD. Drak2*$^{-/-}$ and NOD mice (Figures 6H and S5D), *NOD. Drak2*$^{-/-}$ mice had a greater increase in the number of thymic $T_{regs}$ than NOD mice following IL-2/anti-IL2 complex injection (Figure 6H). Together, these results establish a previously unknown role for DRAK2 in regulating IL-2 signaling and $T_{reg}$ development.

### DRAK2 reduces phosphorylation of STAT5A

As *Drak2*$^{-/-}$ thymocytes had increased STAT5A Y694 phosphorylation following IL-2 stimulation (Figure 6), we investigated whether DRAK2 inhibits JAK-mediated phosphorylation of STAT5A. To eliminate other potential protein interactions, we performed *in vitro* kinase assays with combinations of recombinant JAK1, STAT5A, and DRAK2, followed by liquid chromatography-tandem mass spectrometry (LC-MS/MS). Equal amounts of each protein were incubated in kinase buffer and ATP for 30 min. Reactions were separated by SDS page and analyzed by LC-MS/MS targeting STAT5A Y694. To quantitatively evaluate the absolute abundance of phosphorylated STAT5A Y694, we used the AQUA (absolute quantification) method, which utilizes isotope-labeled peptides corresponding to the unmodified and phosphorylated tryptic STAT5A Y694 peptides that serve as internal standard controls.[37] As expected, STAT5A Y694 was not phosphorylated in the absence of JAK1 and was phosphorylated with addition of JAK1 (Figure 7A). Interestingly, phosphorylation of STAT5A Y694 significantly decreased with the addition of DRAK2, indicating that DRAK2 inhibits JAK1-mediated phosphorylation of STAT5A Y694 (Figure 7A). Importantly, in the absence of JAK1, DRAK2 did not phosphorylate STAT5A Y694, which was expected since DRAK2 is a serine/threonine kinase. DRAK2 may inhibit STAT5A phosphorylation by blocking the interaction of JAK1 and STAT5A by binding to either protein. In addition, DRAK2 may phosphorylate STAT5A S780, which has been shown to inhibit STAT5A activation.[34,38,39] Therefore, we examined relative levels of unmodified and phosphorylated STAT5A S780 in the samples via untargeted LC-MS/MS. We found that relative abundance of phosphorylated STAT5A S780 was increased in the presence of DRAK2, suggesting that DRAK2 may phosphorylate STAT5A S780 (Figure 7B). Together, these data indicate that DRAK2 inhibits JAK1-mediated phosphorylation of STAT5A Y694 and potentially phosphorylates STAT5A S780, which decreases STAT5A activation. Overall, our data reveal a previously unknown mechanism regulating $T_{reg}$ development in which DRAK2 regulates IL-2 signaling in thymocytes. Moreover, our data highlight that DRAK2 impacts susceptibility to autoimmunity via multiple mechanisms.

## DISCUSSION

DRAK2 illustrates the potential of targeting signaling pathways to specifically inhibit autoreactive T cells, while sparing immunity to pathogens and tumors. To further understand the role of DRAK2 in autoimmunity and identify other molecules in this pathway, it is important to define cell types in which DRAK2 signaling impacts T1D development. Although stimulation induced *Drak2* expression in pancreatic β cells, and ectopic *Drak2* expression promoted β-islet cell apoptosis and impaired glucose tolerance,[17,27] we show here that *Drak2* expression in β-islet cells did not impact susceptibility to T1D in the *NOD* model. Rather, *Drak2* deficiency within T cells was sufficient to confer resistance to T1D, as was demonstrated previously in the EAE model.[12] Thus, *Drak2* expression within T cells contributes to disease in two distinct models of autoimmunity.

Our data demonstrate that DRAK2 influences T1D development by regulating multiple mechanisms, which impact both effector T cells and $T_{regs}$. First, we show that DRAK2 functions within conventional T cells to alter sensitivity to $T_{reg}$-mediated suppression. We and others previously demonstrated that *Drak2*$^{-/-}$ effector T cells were more susceptible to apoptosis.[12,22] However, in the absence of $T_{regs}$, *Drak2*$^{-/-}$ conventional T cells induced T1D to a similar extent as wild-type conventional T cells, indicating that increased susceptibility to apoptosis in *Drak2*$^{-/-}$ conventional T cells was not sufficient to prevent autoimmunity. Nevertheless, fewer $T_{regs}$ were required to inhibit *Drak2*$^{-/-}$ conventional T cells compared with wild-type conventional T cells, demonstrating that *Drak2*$^{-/-}$ conventional T cells were more sensitive to $T_{reg}$-mediated suppression. Thus, although $T_{regs}$ are required for disease resistance in *NOD. Drak2*$^{-/-}$mice, DRAK2 impacts T1D incidence by functioning within conventional T cells, rendering them less susceptible to $T_{reg}$-mediated suppression. $T_{regs}$ suppress conventional T cells through multiple mechanisms, including suppressive cytokine secretion, cytokine consumption, cytotoxicity induction, or impairment of antigen presentation.[40,41] The increased sensitivity of *Drak2*$^{-/-}$ conventional T cells to $T_{reg}$ suppression is likely related to the enhanced susceptibility to apoptosis of *Drak2*$^{-/-}$ T cells. In addition, enhanced IL-2 sensitivity in effector T cells may render T cells more susceptible to activation-induced cell death. Interestingly, conventional T cells from T1D patients and *NOD* mice display resistance to $T_{reg}$ suppression.[42] Thus, DRAK2 inhibition may provide an avenue to overcome this resistance.

DRAK2 also impacts T1D by regulating IL-2 signaling in thymocytes. This finding was unexpected as previous data demonstrated that *Drak2*$^{-/-}$ T cells exhibited increased activation, MAPK signaling, proliferation, and cytokine production after sub-optimal stimulation relative to wild-type T cells, suggesting that DRAK2 negatively regulates TCR signaling.[11] However, we show here that Nur77-GFP MFI was similar in developing thymocytes and mature T cells from wild-type and *Drak2*$^{-/-}$ mice, regardless of stimulation level, indicating that DRAK2 is not regulating signals directly downstream of the TCR. Rather, our data reveal that DRAK2 regulates T cell activation by altering the sensitivity to IL-2 signaling.

Our findings further show that altered IL-2 sensitivity impacted $T_{reg}$ development in *Drak2*$^{-/-}$ mice. Both $T_{reg}$ precursor populations in *Drak2*$^{-/-}$ mice exhibited enhanced phosphorylation of STAT5A following IL-2 stimulation compared with wild-type thymocytes. Although the increase in STAT5A phosphorylation was modest in *Drak2*$^{-/-}$ thymocytes, it led to a greater number and proportion of $T_{regs}$ *in vivo* and *in vitro* compared with wild-type thymocytes. *NOD. Drak2*$^{-/-}$ mice also had a small, but significant, increase in Foxp3$^{lo}$ $T_{reg}$ precursors compared with wild-type *NOD* mice, suggesting DRAK2 may impact the development of Foxp3$^{lo}$ precursors. Development of both mature $T_{regs}$ and Foxp3$^{lo}$ precursors requires induction of *Foxp3* expression, which is downstream of IL-2 signaling. Thus, it is possible that DRAK2 regulates the development of both subsets. It is not known if enhanced IL-2 sensitivity increases the generation of Foxp3$^{lo}$ precursors, as these cells develop even in the absence of IL-2 and are also sensitive to IL-4 signaling to drive maturation.[28,43] Alternatively, DRAK2 may uniquely regulate the transition of CD25$^{+}$ precursor to mature $T_{reg}$. Thus, in the absence of *Drak2*, more CD25$^{+}$ precursors would transition to mature $T_{regs}$ compared with Foxp3$^{lo}$ precursors. Since CD25$^{+}$ precursors have a competitive advantage over Foxp3$^{lo}$ precursors for IL-2, the Foxp3$^{lo}$ precursors may accumulate in *Drak2*$^{-/-}$ mice because they have a limited capacity to bind IL-2 and transition to mature $T_{regs}$. Maturation of CD25$^{+}$ precursors and Foxp3$^{lo}$ precursors is mediated by distinct enhancers and gives rise to $T_{regs}$ with differential gene expression and TCR repertoires.[28] Importantly, $T_{regs}$ that mature from CD25$^{+}$ $T_{reg}$ precursors, but not from Foxp3$^{lo}$ precursors, are protective against EAE,[28] high-lighting an additional potential mechanism by which DRAK2 could regulate autoimmunity. Together, our data demonstrate that the absence of *Drak2* in thymocytes increased IL-2 sensitivity and enhanced development of $T_{regs}$. We hypothesize that the modest increase in $T_{regs}$, combined with the elevated susceptibility of *Drak2*$^{-/-}$ effector T cells to $T_{reg}$ suppression, impacts T1D development.

Our data demonstrate a previously unknown role of DRAK2 in regulating IL-2 signaling. Engagement of IL-2 and the IL-2R complex leads to activation of STAT5A via JAK-mediated phosphorylation of STAT5A Y694.[34] We demonstrated that *Drak2*$^{-/-}$ $T_{reg}$ precursors exhibited increased STAT5A Y694 phosphorylation compared with wild-type thymocytes. In addition, an *in vitro* kinase assay showed that DRAK2 inhibited JAK1-mediated phosphorylation of STAT5A Y694. DRAK2 may inhibit STAT5 activation by blocking the JAK and STAT5 interaction. Alternatively, our data also suggest that DRAK2 phosphorylates STAT5A S780, which has been linked to reduced STAT5A activation.[34,38,39] In hepatocytes, DRAK2 inhibits phosphorylation of splicing factor SRSF6 by blocking the kinase and substrate interaction.[18] Furthermore, inhibition of CDK8 and CDK19 in effector T cells reduced phosphorylation of STAT5B S730, which increased tyrosine phosphorylation of STAT5B and enhanced *Foxp3* expression, resulting in a greater number of $T_{regs}$.[39] Thus, DRAK2 may regulate STAT5A activation through similar mechanisms.

Low-dose IL-2 therapy to enhance $T_{reg}$ development has been explored as a therapy for autoimmune disease.[44–47] Indeed, IL-2 treatment protects *NOD* mice from T1D.[48] However, low-dose IL-2 in patients with T1D does not consistently improve clinical outcomes, despite increased $T_{reg}$ abundance, partly due to expanded cytotoxic T cells.[49] Furthermore, combinations of $T_{reg}$ transfer, IL-2 supplementation, islet transfer, or targeted immunosuppression have had limited success.[3,45,47,50,51] Since the absence of *Drak2* increases the prevalence of $T_{regs}$ in tandem with enhanced susceptibility of conventional T cells to $T_{reg}$-mediated suppression, modulating the DRAK2 pathway may enable $T_{reg}$ expansion without increasing cytotoxic T cells.

Overall, our data reveal that DRAK2 impacts T1D development by regulating the susceptibility of conventional T cells to $T_{reg}$-mediated suppression, and by controlling IL-2 sensitivity in thymocytes to modulate the development of $T_{regs}$. As DRAK2 may not inhibit all aspects of the IL-2 signaling pathway, DRAK2 inhibition presents an innovative avenue to increase IL-2 sensitivity within $T_{regs}$ to augment $T_{reg}$ development, while simultaneously enhancing the sensitivity of conventional T cells to $T_{reg}$-mediated suppression.

### Limitations of the study

Our data demonstrate that DRAK2 inhibits phosphorylation of STAT5A, which results in enhanced sensitivity to IL-2 in $T_{reg}$ precursors in the absence of DRAK2. Future experiments will be required to investigate if DRAK2 regulates IL-2 sensitivity specifically in developing thymocytes, or if it also impacts peripheral T cells after activation. In addition, it will be important to examine whether increased susceptibility of *Drak2*$^{-/-}$ conventional T cells to $T_{reg}$-mediated suppression is due to enhanced IL-2 sensitivity and activation-induced cell death. It will also be essential to investigate if DRAK2 inhibits STAT5A activation by blocking JAK and STAT5A interaction, phosphorylating STAT5A S780, or both.

## STAR★METHODS

### RESOURCE AVAILABILITY

**Lead contact—**Further information and requests for resources and reagents should be directed to and will be fulfilled by the lead contact, Maureen McGargill (Maureen.mcgargill@stjude.org).

**Materials availability—**This study did not generate new unique reagents.

#### Data and code availability

- Microarray data have been deposited at NCBI GEO: GSE210853 and are publicly available as of the date of publication.
- The mass spectrometry proteomics data have been deposited to the ProteomeXchange Consortium via the PRIDE partner repository; ProteomeXchange: PXD037922.
- All data reported in this paper will be shared by the lead contact upon request.
- This paper does not report original custom code.
- Any additional information required to reanalyze the data reported in this paper is available from the lead contact upon request.

### EXPERIMENTAL MODEL AND SUBJECT DETAILS

**Mice—***C57BL/6. Drak2*$^{-/-}$ mice were previously described[11] and backcrossed 19 generations to *C57BL/6* mice. *OT-II* mice were obtained from Kristin Hogquist and *C57BL/6.CD45.1, C57BL/6.OT-I*, and *C57BL/6.Nur77*$^{GFP}$ mice were purchased from the Jackson Laboratory and crossed to *C57BL/6. Drak2*$^{-/-}$ mice in house. SNP analysis with Illumina Low Density Linkage Panels showed that greater than 99.0% of the SNPs in the *C57BL/6.*

*Drak2*$^{-/-}$ strains were *C57BL/6. NOD. Drak2*$^{-/-}$ and *NOD.BDC2.5. Drak2*$^{-/-}$ mice were also previously described.[12] *NOD. Drak2*$^{-/-}$ mice were crossed to the *NOD* background for greater than 11 generations. SNP analysis showed that greater than 99.3% of the SNPs in *NOD. Drak2*$^{-/-}$ mice were of *NOD* origin. *NOD.SCID* mice were purchased from the Jackson Laboratory and bred to *NOD. Drak2*$^{-/-}$ *Drak2*$^{-/-}$ *Drak2*$^{-/-}$ *Drak2*$^{-/-}$ mice in house. SNP analysis showed 99.8% of SNPs were from the *NOD* background. All animal studies utilized female mice 4–12 weeks of age, unless otherwise noted. Mice were maintained under specific pathogen-free conditions at St. Jude Children's Research Hospital. Animal studies met the approval of the Animal Ethics Committee.

## METHOD DETAILS

**FACS purification of lymphoid populations—**T cells were purified from spleen and lymph nodes of mice by FAC sorting with antibodies specific for CD4 (RM4–5), CD8 (53–6.7), CD25 (PC61.5), CD44 (IM7), CD45RB (C363–16A), and CD62L (MEL-14). Naive T cells were either $CD25^{-}CD44^{lo}$ or $CD25CD44^{lo}CD62L^{hi}$. Regulatory T cells were $CD4^{+}CD25^{+}CD45RB^{lo}$. Cell sorting was performed using the iCyt Reflection or SY3200 Cell Sorters (Sony Biotechnology). Purity of sorted cells was confirmed via flow cytometry and greater than 94% in all experiments.

**Magnetic separation of T cells—**T cells were purified from lymph nodes and spleen of mice by negative selection with biotin-conjugated antibodies specific for B220, CD11b, CD49b and MHC class II (eBioscience), followed by separation with streptavidin-conjugated magnetic beads (Miltenyi Biotec) on an autoMACS pro separator (Miltenyi Biotec). $CD4^{+}$ and $CD8^{+}$ T cells were purified by negative selection through addition of biotin-conjugated antibodies specific for CD8 or CD4 (eBioscience), respectively, prior to separation.

**T cell adoptive transfer—**T cells were purified via either FAC sorting or magnetic separation from spleen and lymph nodes and injected intravenously via tail vein. The number of polyclonal T cells injected ranged from $3.5–15 \times 10^{6}$/mouse. Blood glucose was monitored at least weekly by testing a drop of venous tail blood with a OneTouch Ultra (Lifescan Inc.) or Bayer Contour® (Ascensia Diabetes Care) blood glucose meter. Mice were considered diabetic after two consecutive readings at least one day apart of 300 mg/dL or greater. For experiments with BDC2.5 TCR transgenic T cells, naive, conventional T cells ($CD4^{+}CD25^{-}CD44^{lo}CD62L^{hi}$) were purified from *NOD.BDC2.5* or *NOD.Drak2*$^{-/-}$*.BDC2.5* (Thy1.1/Thy1.2) mice. 7,500 BDC2.5 T cells were transferred into *NOD.SCID* mice (Thy1.2) with increasing amounts of $T_{regs}$ ($CD4^{+}CD25^{+}CD45RB^{lo}$) that were purified from *NOD* mice (Thy1.1).

**Flow cytometric analysis—**Single cell suspensions of organs were stained with antibodies and analyzed on a FACSCalibur (BD Biosciences), LSR Fortessa (BD Biosciences), or an Aurora spectral cytometer (Cytek). Analysis was performed with FlowJo software (BD Biosciences). For $T_{reg}$ identification, suspensions were stained with antibodies specific for CD4, CD8, and CD25. Additional antibodies included CD44, CD62L, CD69 (FN50), CD122 (TM-β1), CD132 (TUGm2), Helios (22F6), GITR (DTA-1), or CTLA-4

(UC10–4B9). Cells were then fixed and permeabilized with the Foxp3/Transcription Factor Staining Buffer Set according to manufacturer's instructions (eBioscience) and stained with anti-Foxp3 (FJK-16S) antibody.

**Phosflow analysis—**For analysis of phosphorylated STAT5 in thymocytes and peripheral $CD4^+$ T cells, single cell suspensions were rested in complete media (RPMI advanced media, 10% FCS, HEPES, Pen-Strep, L-glutamine, βME, gentamicin) for 30 min at 37°C, then incubated with 0–20 ng/mL recombinant mouse IL-2 (Tonbo biosciences) or 100 ng/mL recombinant mouse IL-4, IL-7, or IL-15 (Invitrogen, R&D systems) for an additional 15 min at 37°C. Cells were immediately fixed and stained for Foxp3 and pSTAT5 using a protocol adapted from Li and Park.[57] Briefly, cells were fixed and stained with the Foxp3/Transcription Factor Staining Buffer Set (eBioscience) according to manufacturer's instructions. Cells were subsequently incubated on ice in 2% paraformaldehyde for 30 min followed by 90% methanol for 30 min. Finally, cells were stained with anti-pSTAT5 (Stat5(pY694), clone 47) for 20 min, followed by surface antibodies for 40 min at room temperature. Cells were then washed and analyzed by flow cytometry. To analyze phosphorylated STAT5 in peripheral $CD8^+$ T cells, cells were purified from the spleen and lymph nodes of female *C57BL/6* mice, stimulated with increasing concentrations of IL-2 for 15 min, then fixed and stained with anti-pSTAT5 (C71E5) using BD Phosflow Fix Buffer I and BD Phosflow Perm Buffer III (BD Biosciences) according to manufacturer's instructions.

**$T_{reg}$ induction—**For in vitro induction, naive *OT-II* and *OT-II.Drak2*$^{-/-}$ ($CD4^+CD25^-CD44^{lo}$) T cells were purified from spleens and lymph nodes of male mice and stimulated with irradiated splenocytes (2500 rads) loaded with 10 μM $OVA_{323–339}$ peptide, (synthesized at the Hartwell Center at St. Jude Children's Research Hospital) for 72 h with increasing amounts of TGF-β (R&D Systems and Cell Signaling). For *in vivo* $T_{reg}$ induction, naive *OT-II* (CD45.1/CD45.2) and *OT-II.Drak2*$^{-/-}$ (CD45.2) T cells were sorted from male mice and combined at a one to one ratio. Two million total T cells were transferred intravenously into CD45.1 host mice. The following day, host mice were given water or water containing 2% ovalbumin for five days, *ad libitum*. Organs were harvested on day six and analyzed by flow cytometry.

**Nur77 stimulation experiments—**Single cell suspensions were prepared from spleens harvested from male *OT-I.Nur77*$^{GFP}$ or *OT-I.Drak2*$^{-/-}$*.Nur77*$^{GFP}$ mice at approximately eight weeks of age. $CD8^+$ T cells were purified via negative selection as described above. Antigen-presenting cells were prepared from a single cell solution of splenocytes from a *CD45.1/1* mouse, irradiated at 2500 rads and pulsed with varying concentrations of OVA-$G4_{257–264}$ or $OVA_{257–264}$ peptide (synthesized at the Hartwell Center at St. Jude Children's Research Hospital) for 1 h at 37°C. T cells and APCs were cultured at a 1:4 ratio in a round bottom 96 well plate for 6 h at 37°C with 10 μg/mL anti-IL2 (JES6–1-A12). Nur77-GFP MFI was determined via flow cytometry following surface staining of $CD8^+$ T cells.

**IL-2 stimulation experiments—**Single cell suspensions were prepared from the thymii of one-day-old *NOD.Drak2*$^{+/-}$ and *NOD.Drak2*$^{-/-}$ mice. Thymocytes were cultured for 24 h in media with increasing concentrations of IL-2 (BD Biosciences). Following stimulation, cells were stained for $T_{reg}$ analysis as described above and analyzed via flow cytometry.

***In vitro* $T_{reg}$ suppression—**Single cell suspensions from spleen and lymph nodes were prepared and depleted of B cells using anti-CD45R/B220 magnetic beads (Miltenyi Biotec). Enriched T cells were subsequently FACS-sorted for naive, conventional T cells (Thy1.1, $CD4^+CD25^-CD44^{lo}CD62L^{hi}$) and *NOD* and *NOD.Drak2*$^{-/-}$ $T_{regs}$ (Thy1.2, $CD4^+CD25^+CD45RB^{lo}$). Conventional cells were then labeled with 5,6-carboxyfluorescein diacetate succinimidyl ester (CFSE) (ThermoFisher Scientific) at 0.25 μM in pre-warmed PBS containing 0.1% FCS for 10 min at 37°C, then washed twice with RPMI advanced media (RPMI advanced media, 10% FCS, HEPES, Pen-Strep, L-glutamine, BME, gentamicin). Next, 50,000 labeled cells were stimulated with 15,000 anti-CD3/CD28-coated T-Activator Dynabeads per well (0.3:1 beads/effector T cell ratio; ThermoFisher Scientific). Naive conventional T cells were stimulated alone or with indicated ratios of *NOD* or *NOD.Drak2*$^{-/-}$ $T_{regs}$ for 72 h. Conventional T cell proliferation was determined by measuring CFSE dilution of viable cells. Cell viability was analyzed using fixable viability dye (eBioscience).

***In vivo* $T_{reg}$ suppression—**Single cell suspensions from the spleen and lymph nodes of *NOD* mice (Thy1.1/Thy1.2) were sorted via FACS for naive ($CD4^+CD25^-CD44^{lo}$) T cells, labeled with 0.25 μM CFSE, and transferred intravenously into *NOD.SCID* mice (Thy1.2) with or without *NOD* or *NOD.Drak2*$^{-/-}$ $T_{regs}$ (Thy1.1) ($CD4^+CD25^+CD45RB^{lo}$) at a ratio of four to one. Lymph nodes were harvested seven days after injection and analyzed for effector T cell proliferation via flow cytometry to determine $T_{reg}$ suppression. Transferred cells were differentiated from host cells by expression of Thy1.1 (HIS51) and Thy1.2 (30-H12).

***In vivo* $T_{reg}$ expansion—**IL-2/anti-IL-2 complexes were prepared by incubating recombinant mouse IL-2 (Tonbo biosciences) and anti-IL-2 (JES6-A12; BioXCell) at a 1:5 ratio for 30 min at 37°C.[36] Complexes were injected interperitoneally into four-week-old *NOD* and *NOD.Drak2*$^{-/-}$ mice, daily for three days. As a control, additional *NOD* and *NOD.Drak2*$^{-/-}$ mice received PBS injections. Five days after the initial injection, thymii and lymph nodes were harvested, and cells were stained to determine $T_{reg}$ abundance via flow cytometry as described above.

**Microarray analysis—**$T_{regs}$ were purified by flow cytometry from the lymph nodes of 4- to 8-week-old *NOD* and *NOD.Drak2*$^{-/-}$ mice based on $CD8CD4^+CD25^+CD45RB^{lo}$ expression. Purity was assessed after the sort via flow cytometry and intracellular Foxp3 expression. The sorted populations were 94–98% $CD4^+Foxp3^+$. Total RNA was extracted using the Qiagen RNeasy micro kit, assessed for quality using the Bioanalyzer 2100, and assessed for quantity using the Nanodrop. 125ng of intact, high-quality RNA was processed using the Thermo Fisher (Affymetrix) Whole Transcript (WT) Plus assay kit and hybridized on the Clariom S mouse array for 16 h at 45°C while rotating at 60rpm. Cartridges were stained and washed on the Gene Chip FS450 fluidics station and then scanned on the Gene Chip Scanner 3000 7G. Resulting Cel files were analyzed using the *oligo* package[56] in

R, differential expression was determined using the *limma* package,[55] and figures were generated using the *ggplot2* package.[54]

***In vitro* kinase assay—**Combinations of recombinant human JAK1 (ThermoFisher), DRAK2 (ThermoFisher), and STAT5A (Abcam) were mixed in equal amounts. The *in vitro* kinase reaction was carried out in kinase reaction buffer (10 mM $MgCl_2$, 3 mM $MnCl_2$, 10 mM Tris-HCl, pH 7.2) in the presence or absence of 20 μM ATP for 10 min at 30°C, as previously described.[10] Reactions were terminated by snap freezing in liquid nitrogen.

**Proteomics analysis by liquid chromatography-tandem mass spectrometry (LC-MS/MS)—**Proteomics analysis was based on a previously optimized protocol with minor modifications.[58] Briefly, the *in vitro* kinase assay reactions were resolved on a 10% SDS-PAGE gel and proteins were in-gel digested, peptides extracted and divided into two equimolar aliquots (v/v), with one aliquot used for Absolute Quantification (AQUA) experiments. Peptides were fractionated on a CoAnn 75 μm × 20 cm C18 column with 1.9 μm resin (heat at 50°C) using a 30 min gradient of 10%–40% buffer B (70% ACN, 2.5% DMSO, and 0.1% FA) at an optimal flow rate of ~0.33 μL/min using a Dionex Ultimate 3000 ultra-high pressure liquid chromatography (UHPLC) system connected in-line to a Fusion mass spectrometer (Thermo Fisher Scientific). The mass spectrometer was operated in a “high-high” (FTMS-HCD-FTMS) data-dependent mode, with a survey scan in Orbitrap (60,000 resolution, scan range 300–2000 m/z, $1 \times 10^6$ AGC target, ~100 ms maximal ion time), followed by up to 20 data-dependent (15,000 resolution, scan range 120–1200 m/z, $1 \times 10^6$ AGC target, ~150 ms maximal ion time).

Synthetic Peptides Assay Development and Absolute Quantification (AQUA) Proteomics: the AQUA (heavy Glycine-labeled) STAT5A Y694 peptides with unmodified Y694 (AVDGYVKPQIK) or Phospho-Y694 (AVDGYVKPQIK) were synthesized at the Hartwell center and HPLC-purified. The two synthetic peptides were used to evaluate LC retention time, MS detection sensitivity, and MS/MS spectra. Absolute Quantification (AQUA) proteomics were performed using AQUA peptides spiked-in at equimolar ratio (Phos AQUA/Non-Phos AQUA ratio = 1/1) and acquired on a Fusion mass spectrometer (Thermo Fisher Scientific) operating in targeted high-resolution MS/MS mode.

The MS/MS data were computationally processed by converting the MS/MS raw files to mzXML files (ProteoWizard 3.0.22198-e6bb91f 64-bit) followed by PEAKS Studio 10.6 (Build 20201221, Bioinformatics Solutions Inc.) software search against the UniProt human database (validated, revision, 2021.09.12; entries: 20948).[52,59] Major parameters included precursor and product ion mass tolerance (± 25 ppm, 0.1 Da), fully tryptic, static mass shift for carbamidomethyl modification of cysteine (+57.02146), dynamic mass shift for oxidation of Methionine (+15.99491), for Phosphorylation of Serine, Threonine, and Tyrosine residues (+79.96633), and Glycine heavy-isotope label (+2.0067); maximal missed cleavage (n = 3), and maximal modification sites (n = 3). All matched MS/MS spectra were filtered by mass accuracy and matching scores to reduce protein false discovery rate to ~1% based on the target/decoy search strategy.[60] Peptide assignments and modification sites were further analyzed by Ascore, de novo sequencing for the manual assignment of site-specific fragment ions, and by LC retention time comparison against the synthetic AQUA peptide standard. Proteins were quantified by summing the MS1 Peak Area across all matched PSMs using the PEAKS Studio 10.6 and Skyline (21.2.0.536 dbaf6ccd2, 64-bit) software.[53]

### QUANTIFICATION AND STATISTICAL ANALYSIS

Data were analyzed for statistical significance using GraphPad Prism (GraphPad Software). Disease incidence was analyzed with a Log rank (Mantel-Cox) test. Comparisons of two groups were conducted with either Mann-Whitney U tests (two-tailed), two-sample t-tests, or multiple Mann-Whitney or t-tests with the Holm-Šidàk correction. For Nur77-GFP stimulation, IL-2 stimulation, *in vitro* $T_{reg}$ suppression and *in vitro* $T_{reg}$ induction experiments, data were analyzed via two-way ANOVA with a Šidàk multiple testing correction. *In vivo* $T_{reg}$ suppression assays and proteomics analysis were analyzed via one-way ANOVA with a Šidàk multiple testing correction. Further statistical details can be found in the figure legends.

## Supplementary Material

Refer to Web version on PubMed Central for supplementary material.

## ACKNOWLEDGMENTS

The authors thank Benjamin Edwards, Carlessia Lewis, Juan Mejia, and Ashley Castellaw for technical assistance. We thank the Hartwell Center of St. Jude Children's Research Hospital for peptide synthesis. This work was supported in part by the National Cancer Institute of the National Institutes of Health under award no. P30 CA021765, a Juvenile Diabetes Research Foundation Career Development Award to M.A.M., 2-2007-105, and ALSAC.

## INCLUSION AND DIVERSITY

We support inclusive, diverse, and equitable conduct of research.

## REFERENCES

1. Mayer-Davis EJ, Lawrence JM, Dabelea D, Divers J, Isom S, Dolan L, Imperatore G, Linder B, Marcovina S, Pettitt DJ, et al. (2017). Incidence trends of type 1 and type 2 diabetes among youths, 2002–2012. N. Engl. J. Med. 376, 1419–1429. 10.1056/NEJMoa1610187. [PubMed: 28402773]
2. Rogers MAM, Kim C, Banerjee T, and Lee JM (2017). Fluctuationsin the incidence of type 1 diabetes in the United States from 2001 to 2015: a longitudinal study. BMC Med. 15, 199. 10.1186/s12916-017-0958-6. [PubMed: 29115947]
3. Warshauer JT, Bluestone JA, and Anderson MS (2020). New frontiers in the treatment of type 1 diabetes. Cell Metab. 31, 46–61. 10.1016/j.cmet.2019.11.017. [PubMed: 31839487]
4. Office of Women's Health (2019). Autoimmune Diseases. https://www.womenshealth.gov/a-z-topics/autoimmune-diseases.
5. National Diabetes Statistics Report (2020). Estimates of Diabetes and its Burden in the United States, p. 32.
6. Carey IM, Critchley JA, DeWilde S, Harris T, Hosking FJ, and Cook DG (2018). Risk of infection in type 1 and type 2 diabetes compared with the general population: a matched cohort study. Diabetes Care 41, 513–521. 10.2337/dc17-2131. [PubMed: 29330152]
7. Rose NR (2016). Prediction and prevention of autoimmune disease in the 21st century: a review and preview. Am. J. Epidemiol. 183, 403–406. 10.1093/aje/kwv292. [PubMed: 26888748]

8. Burrack AL, Martinov T, and Fife BT (2017). T cell-mediated beta cell destruction: autoimmunity and alloimmunity in the context of type 1 diabetes. Front. Endocrinol 8, 343. 10.3389/fendo.2017.00343.
9. Lorenzo PI, Cobo-Vuilleumier N, Martín-Vázquez E, López-Noriega L, and Gauthier BR (2021). Harnessing the endogenous plasticity of pancreatic islets: a feasible regenerative medicine therapy for diabetes? Int. J. Mol. Sci. 22, 4239. 10.3390/ijms22084239. [PubMed: 33921851]
10. Sanjo H, Kawai T, and Akira S (1998). DRAKs, novel serine/threonine kinases related to death-associated protein kinase that trigger apoptosis. J. Biol. Chem. 273, 29066–29071. 10.1074/jbc.273.44.29066. [PubMed: 9786912]
11. McGargill MA, Wen BG, Walsh CM, and Hedrick SM (2004). A deficiency in Drak2 results in a T cell hypersensitivity and an unexpected resistance to autoimmunity. Immunity 21, 781–791. 10.1016/j.immuni.2004.10.008. [PubMed: 15589167]
12. McGargill MA, Choy C, Wen BG, and Hedrick SM (2008). Drak2 regulates the survival of activated T cells and is required for organ-specific autoimmune disease. J. Immunol. 181, 7593–7605. [PubMed: 19017948]
13. Edwards BA, Harris TL, Floersh H, Lukens JR, Zaki MH, Vogel P,Kanneganti T-D, Bui JD, and McGargill MA (2015). Drak2 is not required for tumor surveillance and suppression. Int. Immunol. 27, 161–166. 10.1093/intimm/dxu146. [PubMed: 25568303]
14. Wang S, Welte T, McGargill M, Town T, Thompson J, Anderson JF,Flavell RA, Fikrig E, Hedrick SM, and Wang T (2008). Drak2 contributes to West Nile virus entry into the brain and lethal encephalitis. J.Immunol.181,2084–2091.10.4049/jimmunol.181.3.2084. [PubMed: 18641347]
15. Ramos SJ, Hardison JL, Stiles LN, Lane TE, and Walsh CM (2007). Anti-viral effector T cell responses and trafficking are not dependent upon DRAK2 signaling following viral infection of the central nervous system. Autoimmunity 40, 54–65. 10.1080/08916930600996700. [PubMed: 17364498]
16. Kuwahara H, Nishizaki M, and Kanazawa H (2008). Nuclear localization signal and phosphorylation of Serine350 specify intracellular localization of DRAK2. J. Biochem. 143, 349–358. 10.1093/jb/mvm236. [PubMed: 18084041]
17. Mao J, Luo H, Han B, Bertrand R, and Wu J (2009). Drak2 is up-stream of p70S6 kinase: its implication in cytokine-induced islet apoptosis, diabetes, and islet transplantation. J. Immunol. 182, 4762–4770. 10.4049/jimmunol.0802255. [PubMed: 19342653]
18. Li Y, Xu J, Lu Y, Bian H, Yang L, Wu H, Zhang X, Zhang B, Xiong M, Chang Y, et al. (2021). DRAK2 aggravates nonalcoholic fatty liver disease progression through SRSF6-associated RNA alternative splicing. Cell Metab. 33, 2004–2020.e9. 10.1016/j.cmet.2021.09.008. [PubMed: 34614409]
19. Park Y, Kim W, Lee J-M, Park J, Cho JK, Pang K, Lee J, Kim D, Park S-W, Yang K-M, and Kim SJ (2015). Cytoplasmic DRAK1 overexpressed in head and neck cancers inhibits TGF-β1 tumor suppressor activity by binding to Smad3 to interrupt its complex formation with Smad4. Oncogene 34, 5037–5045. 10.1038/onc.2014.423. [PubMed: 25531329]
20. Yang K-M, Kim W, Bae E, Gim J, Weist BM, Jung Y, Hyun J-S, Hernandez JB, Leem S-H, Park T, et al. (2012). DRAK2 participates in a negative feedback loop to control TGF-b/Smads signaling by binding to type I TGF-b receptor. Cell Rep. 2, 1286–1299. 10.1016/j.celrep.2012.09.028. [PubMed: 23122956]
21. Harris TL, and McGargill MA (2015). Drak2 does Not regulate TGF-β signaling in T cells. PLoS One 10, e0123650. 10.1371/journal.pone.0123650. [PubMed: 25951457]
22. Ramos SJ, Hernandez JB, Gatzka M, and Walsh CM (2008). Enhanced T cell apoptosis within Drak2-deficient mice promotes resistance to autoimmunity. J. Immunol. 181, 7606–7616. 10.4049/jimmunol.181.11.7606. [PubMed: 19017949]
23. Friedrich ML, Cui M, Hernandez JB, Weist BM, Andersen H-M, Zhang X, Huang L, and Walsh CM (2007). Modulation of DRAK2 autophosphorylation by antigen receptor signaling in primary lymphocytes. J. Biol. Chem. 282, 4573–4584. 10.1074/jbc.M606675200. [PubMed: 17182616]
24. Friedrich ML, Wen BG, Bain G, Kee BL, Katayama C, Murre C, Hedrick SM, and Walsh CM (2005). DRAK2, a lymphoid-enriched DAP kinase, regulates the TCR activation threshold during thymocyte selection. Int. Immunol. 17, 1379–1390. 10.1093/intimm/dxh315. [PubMed: 16172133]

25. Fracchia KM, Pai CY, and Walsh CM (2013). Modulation of T cell metabolism and function through calcium signaling. Front. Immunol. 4, 324. 10.3389/fimmu.2013.00324. [PubMed: 24133495]
26. Kuwahara H, Kamei J.i., Nakamura N, Matsumoto M, Inoue H, and Kanazawa H (2003). The apoptosis-inducing protein kinase DRAK2 is inhibited in a calcium-dependent manner by the calcium-binding protein CHP. J. Biochem. 134, 245–250. 10.1093/jb/mvg137. [PubMed: 12966074]
27. Mao J, Luo H, and Wu J (2008). Drak2 overexpression results in increased beta-cell apoptosis after free fatty acid stimulation. J. Cell. Biochem. 105, 1073–1080. 10.1002/jcb.21910. [PubMed: 18777517]
28. Owen DL, Mahmud SA, Sjaastad LE, Williams JB, Spanier JA, Simeonov DR, Ruscher R, Huang W, Proekt I, Miller CN, et al. (2019). Thymic regulatory T cells arise via two distinct developmental programs. Nat. Immunol. 20, 195–205. 10.1038/s41590-018-0289-6. [PubMed: 30643267]
29. Lio C-WJ, and Hsieh C-S (2008). A two-step process for thymic regulatory T cell development. Immunity 28, 100–111. 10.1016/j.immuni.2007.11.021. [PubMed: 18199417]
30. Klein L, Robey EA, and Hsieh C-S (2019). Central CD4+ T cell tolerance: deletion versus regulatory T cell differentiation. Nat. Rev. Immunol.19, 7–18. 10.1038/s41577-018-0083-6. [PubMed: 30420705]
31. Ashouri JF, and Weiss A (2017). Endogenous Nur77 is a specific indicator of antigen receptor signaling in human T and B cells. J. Immunol. 198, 657–668. 10.4049/jimmunol.1601301. [PubMed: 27940659]
32. Moran AE, Holzapfel KL, Xing Y, Cunningham NR, Maltzman JS, Punt J, and Hogquist KA (2011). T cell receptor signal strength in Treg and iNKT cell development demonstrated by a novel fluorescent reporter mouse. J. Exp. Med. 208, 1279–1289. 10.1084/jem.20110308. [PubMed: 21606508]
33. Owen DL, Sjaastad LE, and Farrar MA (2019). Regulatory T cell development in the thymus. J. Immunol. 203, 2031–2041. 10.4049/jimmunol.1900662. [PubMed: 31591259]
34. Jones DM, Read KA, and Oestreich KJ (2020). Dynamic roles for IL-2–STAT5 signaling in effector and regulatory CD4+ T cell populations. J. Immunol. 205, 1721–1730. 10.4049/jimmunol.2000612. [PubMed: 32958706]
35. Spolski R, Li P, and Leonard WJ (2018). Biology and regulation of IL-2: from molecular mechanisms to human therapy. Nat. Rev. Immunol. 18, 648–659. 10.1038/s41577-018-0046-y. [PubMed: 30089912]
36. Webster KE, Walters S, Kohler RE, Mrkvan T, Boyman O, Surh CD, Grey ST, and Sprent J (2009). In vivo expansion of T reg cells with IL-2–mAb complexes: induction of resistance to EAE and long-term acceptance of islet allografts without immunosuppression. J. Exp. Med. 206, 751–760. 10.1084/jem.20082824. [PubMed: 19332874]
37. Kettenbach AN, Rush J, and Gerber SA (2011). Absolute quantification of protein and post-translational modification abundance with stable isotope–labeled synthetic peptides. Nat. Protoc. 6, 175–186. 10.1038/nprot.2010.196. [PubMed: 21293459]
38. Pircher TJ, Flores-Morales A, Mui AL, Saltiel AR, Norstedt G, Gustafsson J-Å, and Haldosén LA (1997). Mitogen-activated protein kinase kinase inhibition decreases growth hormone stimulated transcription mediated by STAT5. Mol. Cell. Endocrinol. 133, 169–176. 10.1016/S0303-7207(97)00164-0. [PubMed: 9406863]
39. Akamatsu M, Mikami N, Ohkura N, Kawakami R, Kitagawa Y, Sugimoto A, Hirota K, Nakamura N, Ujihara S, Kurosaki T, et al. (2019). Conversion of antigen-specific effector/memory T cells into Foxp3-expressing Treg cells by inhibition of CDK8/19. Sci. Immunol 4, eaaw2707. 10.1126/sciimmunol.aaw2707. [PubMed: 31653719]
40. Mercadante ER, and Lorenz UM (2016). Breaking free of control: how conventional T cells overcome regulatory T cell suppression. Front. Immunol. 7, 193. 10.3389/fimmu.2016.00193. [PubMed: 27242798]
41. Schmidt A, Oberle N, and Krammer PH (2012). Molecular mechanisms of Treg-mediated T cell suppression. Front. Immunol. 3, 51. 10.3389/fimmu.2012.00051. [PubMed: 22566933]

42. Schneider A, Rieck M, Sanda S, Pihoker C, Greenbaum C, and Buckner JH (2008). The effector T cells of diabetic subjects are resistant to regulation via CD4+ FOXP3+ regulatory T cells. J. Immunol. 181, 7350–7355. 10.4049/jimmunol.181.10.7350. [PubMed: 18981158]
43. Marshall D, Sinclair C, Tung S, and Seddon B (2014). Differential requirement for IL-2 and IL-15 during bifurcated development of thymic regulatory T cells. J. Immunol. 193, 5525–5533. 10.4049/jimmunol.1402144. [PubMed: 25348623]
44. Graßhoff H, Comdühr S, Monne LR, Müller A, Lamprecht P, Rieme-kasten G, and Humrich JY (2021). Low-dose IL-2 therapy in autoimmune and rheumatic diseases. Front. Immunol. 12, 648408. 10.3389/fimmu.2021.648408. [PubMed: 33868284]
45. Long SA, Buckner JH, and Greenbaum CJ (2013). IL-2 therapy in type 1 diabetes: "trials" and tribulations. Clin. Immunol. 149, 324–331. 10.1016/j.clim.2013.02.005. [PubMed: 23499139]
46. Rosenzwajg M, Lorenzon R, Cacoub P, Pham HP, Pitoiset F, El Soufi K, RIbet C, Bernard C, Aractingi S, Banneville B, et al. (2019). Immunological and clinical effects of low-dose interleukin-2 across 11 autoimmune diseases in a single, open clinical trial. Ann. Rheum. Dis. 78, 209–217. 10.1136/annrheumdis-2018-214229. [PubMed: 30472651]
47. Bettini M, and Bettini ML (2021). Function, failure, and the future potential of Tregs in type 1 diabetes. Diabetes 70, 1211–1219. 10.2337/dbi18-0058. [PubMed: 34016597]
48. Tang Q, Adams JY, Penaranda C, Melli K, Piaggio E, Sgouroudis E, Piccirillo CA, Salomon BL, and Bluestone JA (2008). Central role of defective interleukin-2 production in the triggering of islet autoimmune destruction. Immunity 28, 687–697. 10.1016/j.immuni.2008.03.016. [PubMed: 18468463]
49. Dong S, Hiam-Galvez KJ, Mowery CT, Herold KC, Gitelman SE,Esensten JH, Liu W, Lares AP, Leinbach AS, Lee M, et al. (2021). The effects of low-dose IL-2 on Treg adoptive cell therapy in patients with Type 1 diabetes. JCI Insight 6, 147474. 10.1172/jci.insight.147474.
50. Hulme MA, Wasserfall CH, Atkinson MA, and Brusko TM (2012). Central role for interleukin-2 in type 1 diabetes. Diabetes 61, 14–22. 10.2337/db11-1213. [PubMed: 22187370]
51. Marfil-Garza BA, Hefler J, Bermudez De Leon M, Pawlick R, Dadheech N, and Shapiro AMJ (2021). Progress in translational tegulatory T cell therapies for type 1 diabetes and islet transplantation. Endocr. Rev. 42, 198–218. 10.1210/endrev/bnaa028. [PubMed: 33247733]
52. Chambers MC, Maclean B, Burke R, Amodei D, Ruderman DL, Neumann S, Gatto L, Fischer B, Pratt B, Egertson J, et al. (2012). A cross-platform toolkit for mass spectrometry and proteomics. Nat. Biotechnol. 30, 918–920. 10.1038/nbt.2377. [PubMed: 23051804]
53. Pino LK, Searle BC, Bollinger JG, Nunn B, MacLean B, and Mac-Coss MJ (2020). The Skyline ecosystem: Informatics for quantitative mass spectrometry proteomics. Mass Spectrom. Rev. 39, 229–244. 10.1002/mas.21540. [PubMed: 28691345]
54. Wickham H, Chang W, Henry L, Pedersen TL, Takahaski K, Wilke C, Woo K, Yutani H, and Dunnington D (2016). ggplot2: Elegant Graphics for Data Analysis, 2nd ed. (Springer-Verlag).
55. Ritchie ME, Phipson B, Wu D, Hu Y, Law CW, Shi W, and Smyth GK (2015). Limma powers differential expression analyses for RNA-sequencing and microarray studies. Nucleic Acids Res. 43, e47. 10.1093/nar/gkv007. [PubMed: 25605792]
56. Carvalho BS, and Irizarry RA (2010). A framework for oligonucleotide microarray preprocessing. Bioinformatics 26, 2363–2367. 10.1093/bioinformatics/btq431. [PubMed: 20688976]
57. Li C, and Park J-H (2020). Assessing IL-2-induced STAT5 phosphorylation in fixed, permeabilized Foxp3+ Treg cells by multiparameter flow cytometry. STAR Protoc. 1, 100195. 10.1016/j.xpro.2020.100195. [PubMed: 33377089]
58. Wang B, Maxwell BA, Joo JH, Gwon Y, Messing J, Mishra A, Shaw TI, Ward AL, Quan H, Sakurada SM, et al. (2019). ULK1 and ULK2 regulate stress Granule Disassembly through phosphorylation and activation of VCP/p97. Mol. Cell 74, 742–757.e8. 10.1016/j.molcel.2019.03.027. [PubMed: 30979586]
59. Zhang J, Xin L, Shan B, Chen W, Xie M, Yuen D, Zhang W, Zhang Z, Lajoie GA, and Ma B (2012). Peaks DB: de novo sequencing assisted database search for sensitive and accurate peptide identification. Mol. Cell. Proteomics 11, M111.010587. 10.1074/mcp.M111.010587.

60. Peng J, Elias JE, Thoreen CC, Licklider LJ, and Gygi SP (2003). Evaluation of multidimensional chromatography coupled with tandem mass spectrometry (LC/LC-MS/MS) for large-scale protein analysis: the yeast proteome. J. Proteome Res. 2, 43–50. 10.1021/pr025556v. [PubMed: 12643542]

## Highlights

- Resistance to type 1 diabetes in *Drak2*-deficient mice requires $T_{regs}$
- DRAK2 alters conventional T cell sensitivity to $T_{reg}$-mediated suppression
- DRAK2 inhibits IL-2 signaling by blocking STAT5 phosphorylation
- Regulation of IL-2 signaling by DRAK2 impacts $T_{reg}$ development

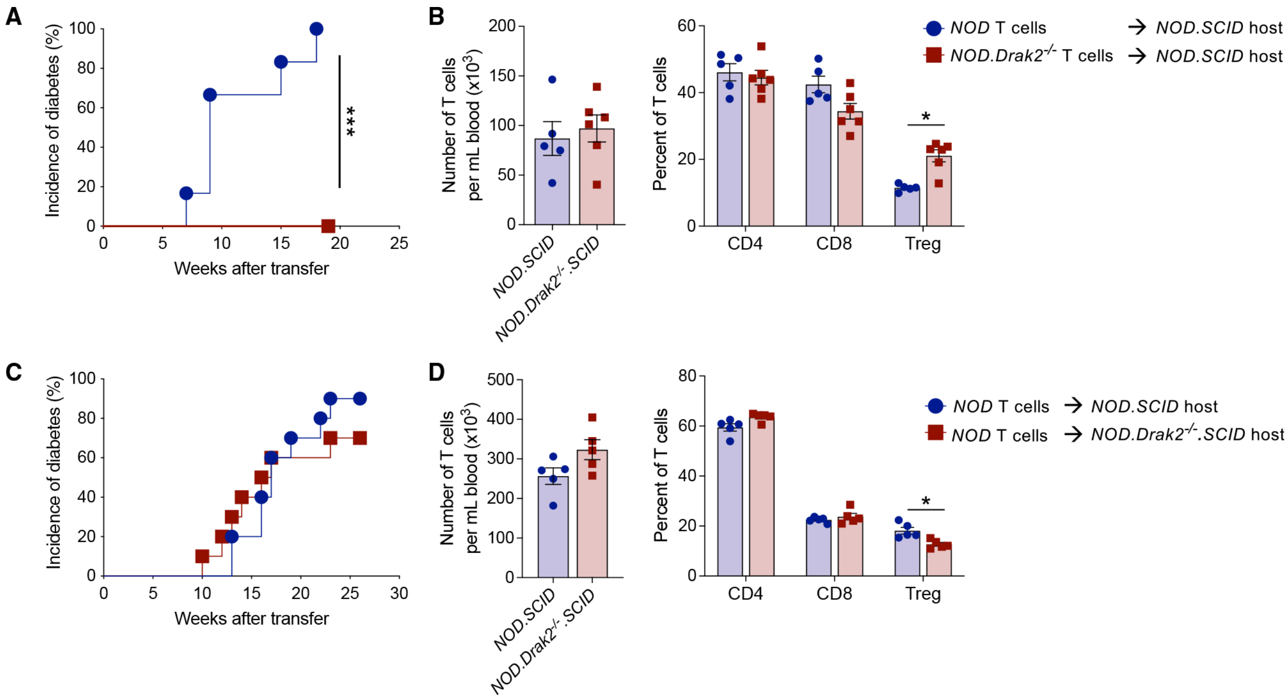


**Figure 1. The resistance to T1D in *NOD.Drak2*$^{-/-}$ mice transfers with T cells and is independent of *Drak2* expression in islet cells**

(A) Purified T cells from *NOD* or *NOD.Drak2*$^{-/-}$ mice were transferred into *NOD.SCID* mice. Blood glucose levels were monitored, and the incidence of diabetes is plotted. Data are representative of two independent experiments with 6–10 mice per group.

(B) Eleven weeks after transfer, the number and proportions of transferred T cells were assessed via flow cytometry.

(C) Purified T cells from *NOD* mice were transferred into *NOD.SCID* or *NOD.Drak2*$^{-/-}$*.SCID* mice, which were monitored for diabetes. Diabetes incidence for 10 mice per group is plotted. Data are combined from two independent experiments.

(D) Seven weeks after transfer, the number and proportions of transferred T cells in the blood were determined by flow cytometry. All mice were 8–12 weeks of age. Data were analyzed with a log rank (Mantel-Cox) test (A and C) or Mann-Whitney tests with the Holm-Šidàk correction (B and D). Error bars represent standard error of the mean. *$p < 0.05$, ***$p < 0.001$.

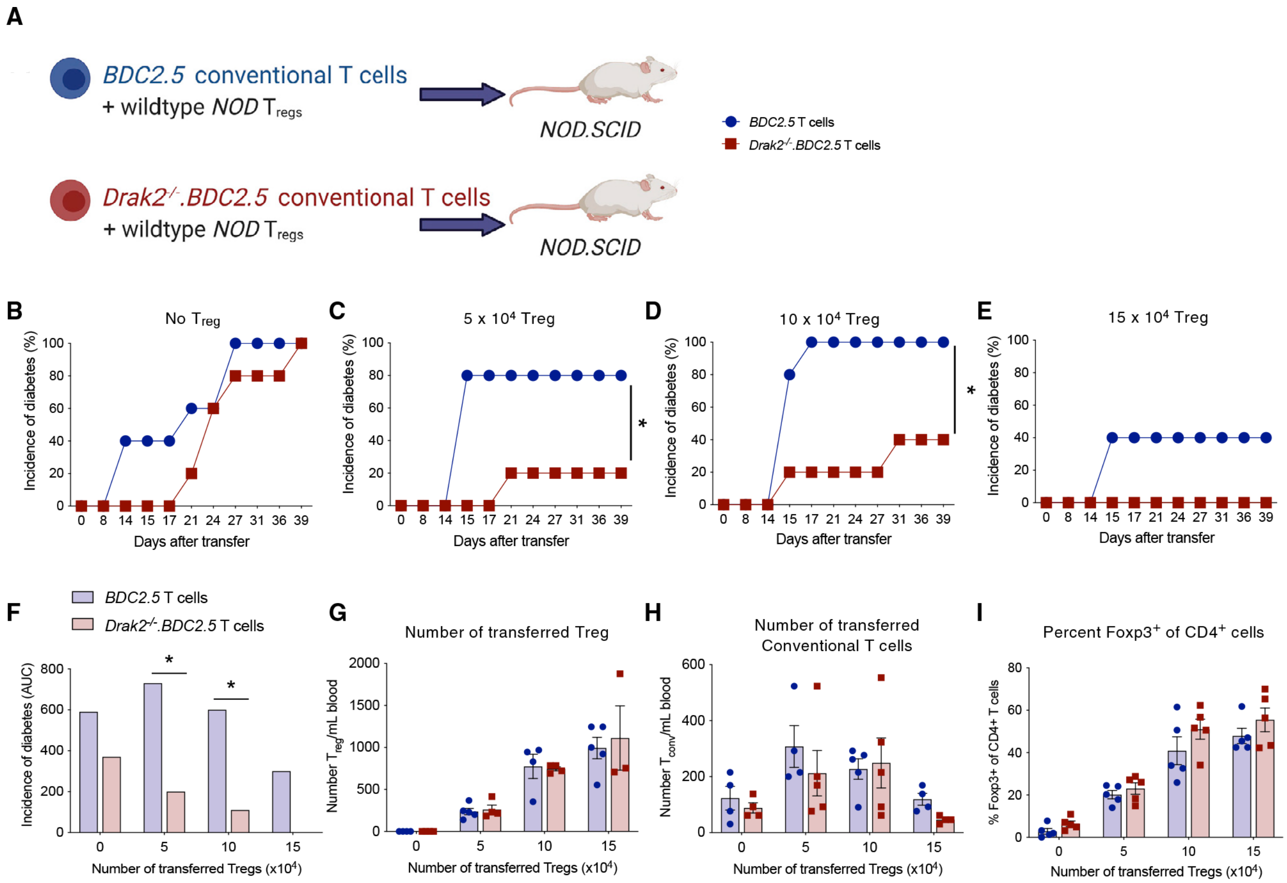


**Figure 2. The resistance to T1D in *NOD.Drak2*$^{-/-}$ mice requires regulatory T cells**

(A–E) Purified, conventional T cells (CD4$^+$CD25$^-$CD44$^{lo}$CD62L$^{hi}$) from 8-week-old *NOD.BDC2.5* or *NOD.Drak2*$^{-/-}$.BDC2.5 mice were transferred into *NOD.SCID* mice with increasing numbers of purified, wild-type *NOD* T$_{regs}$ (CD4$^+$CD25$^+$CD45RB$^{lo}$). Mice were monitored for diabetes via blood glucose levels. Incidence of diabetes in five mice per group receiving (B) no T$_{regs}$, (C) 5 × 10$^4$ T$_{regs}$, (D) 10 × 10$^4$ T$_{regs}$, and (E) 15 × 10$^4$ T$_{regs}$.

(F) Area under the curve (AUC) of diabetes incidence graphs depicted in (B–E). Statistical significance for (B–F) was determined via log rank (Mantel-Cox) test.

(G–I) Eight days after transfer, the number of transferred T$_{regs}$, (H) conventional T cells, and (I) proportion Foxp3$^+$ of CD4$^+$ T cells in blood was assessed via flow cytometry. Data were analyzed via two-way ANOVA with a Šidàk multiple testing correction. Error bars represent standard error of the mean. Data are representative of two independent experiments. *$p < 0.05$. See also Figures S1 and S2.

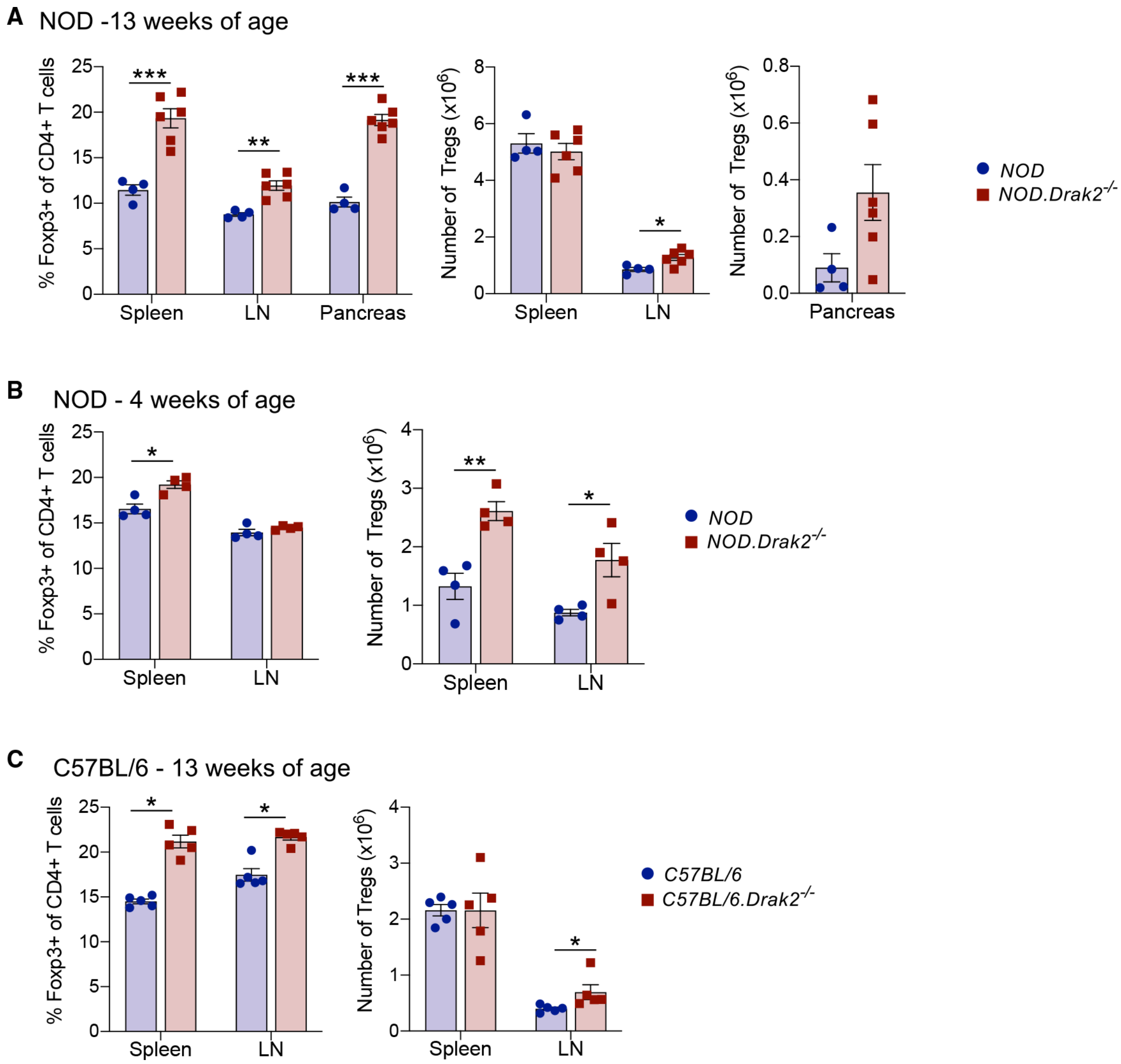


**Figure 3. Drak2$^{-/-}$ mice exhibit an increase in Foxp3$^{+}$CD4$^{+}$ T$_{regs}$ compared with wild-type mice**

(A–C) The number and proportion of T$_{regs}$ in the spleen, lymph nodes, and pancreas of (A) 13-week-old *NOD* mice, (B) 4-week-old *NOD* mice, and (C) 13-week-old *C57BL/6* mice were determined by flow cytometry. Data were analyzed using multiple t tests or Mann-Whitney tests and the Holm-Šidàk correction. Error bars represent standard error of the mean for four to six mice per group and are representative of two to four independent experiments. *p < 0.05, **p < 0.01, ***p < 0.001. See also Figures S3 and S4.

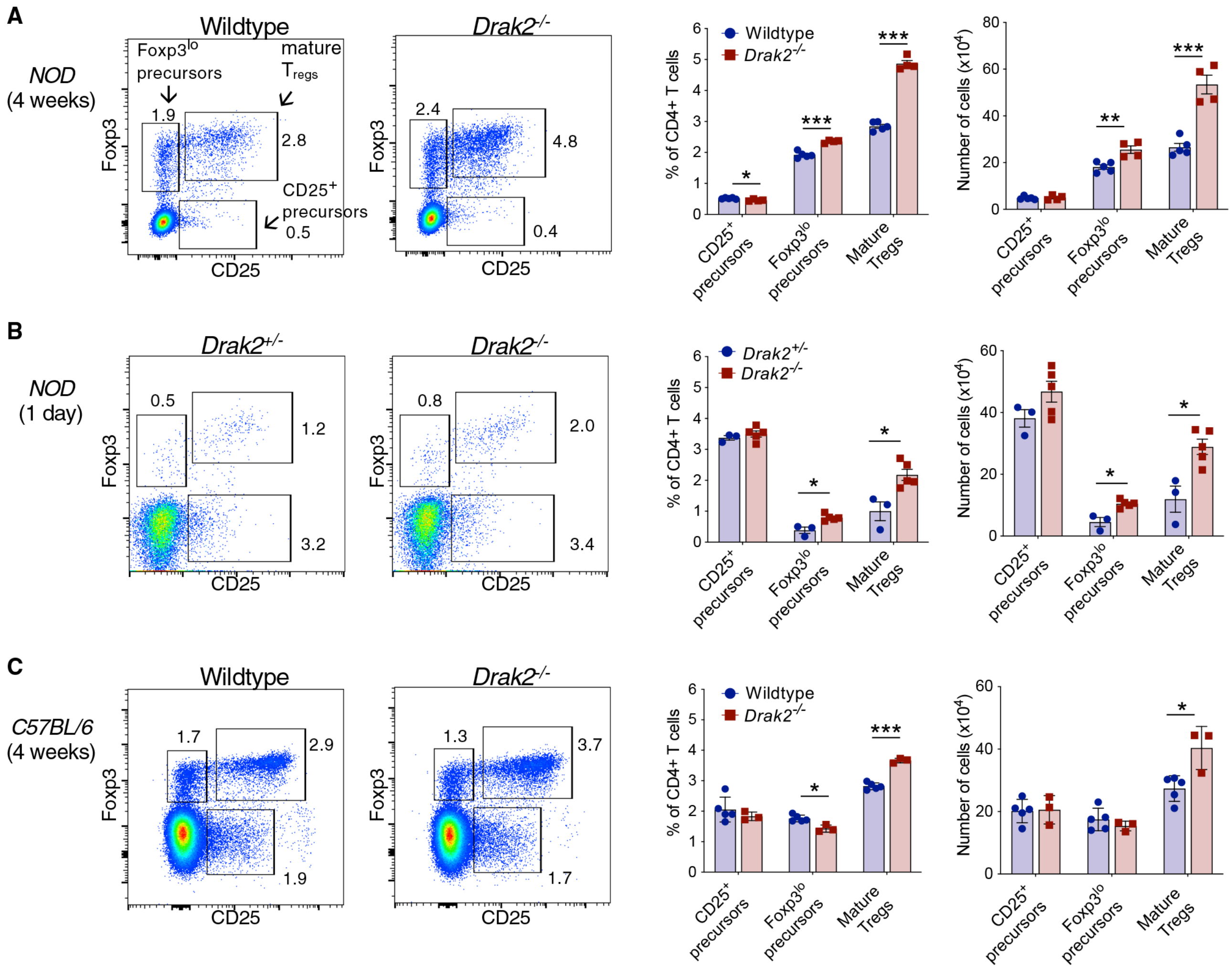


**Figure 4. Thymic $T_{reg}$ development is enhanced in the absence of *Drak2***

(A–C) Cells from thymii of (A) 4-week-old *NOD* and *NOD.Drak2*$^{-/-}$mice, (B) 1-day-old *NOD.Drak2*$^{+/-}$ and *NOD.Drak2*$^{-/-}$ neonates, or (C) 4-week-old *C57BL/6* and *C57BL/6.Drak2*$^{-/-}$ mice were analyzed by flow cytometry. Representative plots of CD25 and Foxp3 gated on viable $CD4^{+}CD8^{-}$ thymocytes are shown with the absolute number and frequency of $CD25^{+}$ precursors ($CD25^{+}Foxp3^{neg}$), $Foxp3^{lo}$ precursors ($CD25^{neg}Foxp3^{lo}$), or mature $T_{regs}$ ($CD25^{+}Foxp3^{+}$) of $CD4^{+}CD8^{-}$ thymocytes. Error bars represent standard error of the mean for three to five mice per group and represent two to four independent experiments. Data were analyzed using multiple t tests with the Holm-Šidàk correction. *$p < 0.05$, **$p < 0.01$, ***$p < 0.001$.

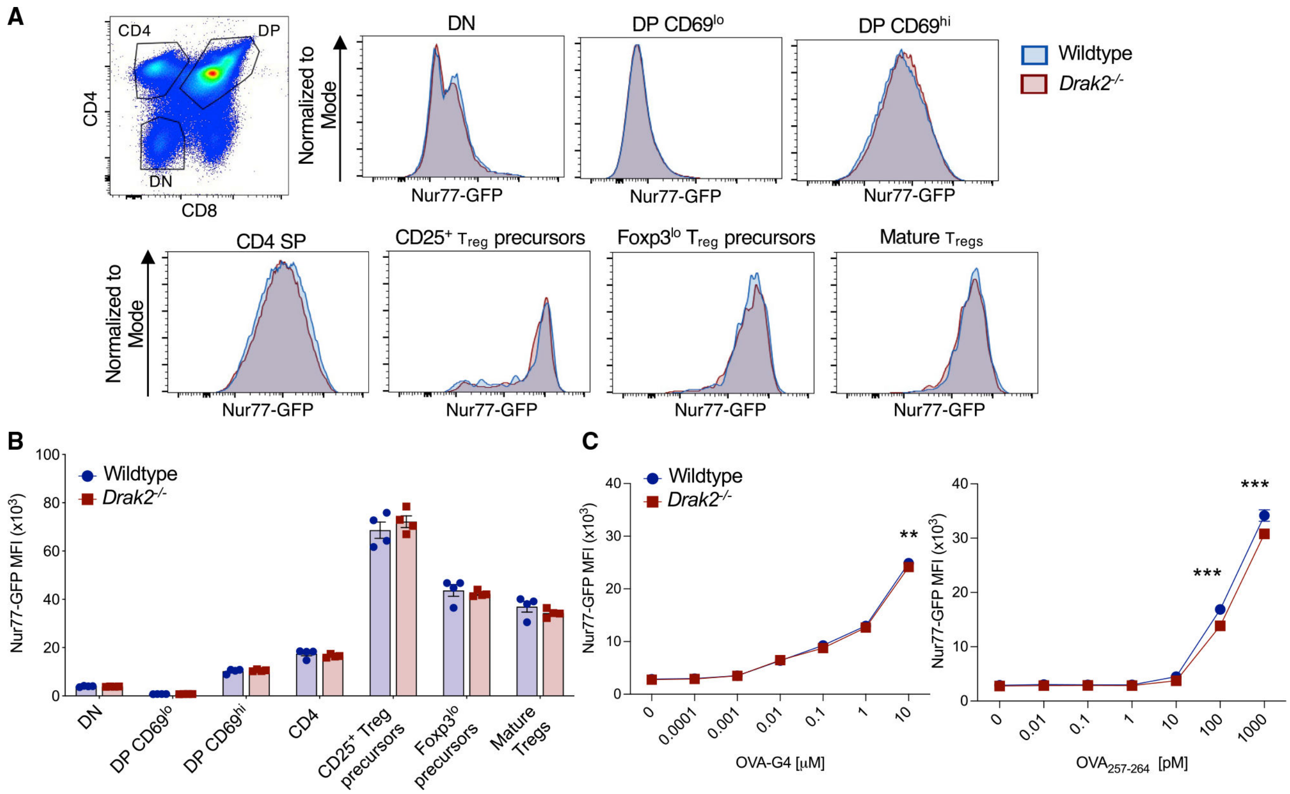


**Figure 5. Drak2$^{-/-}$ T cells exhibit comparable TCR signaling with wild-type T cells**

Thymocytes were harvested from 4- to 6-week-old *C57BL/6.Nur77$^{GFP}$* or *C57BL/6.Drak2$^{-/-}$.Nur77$^{GFP}$* mice and analyzed via flow cytometry.

(A) Gating strategy and representative histograms of Nur77-GFP MFI in CD4$^{-}$CD8$^{-}$ (double-negative [DN]), CD69$^{lo}$ CD4$^{+}$CD8$^{+}$ (double-positive [DP]), CD69$^{hi}$ DP, CD4$^{+}$CD8$^{-}$ (CD4 single-positive [CD4 SP]), CD25$^{+}$ T$_{reg}$ precursors, Foxp3$^{lo}$ T$_{reg}$ precursors, and mature T$_{regs}$.

(B) Nur77-GFP MFI is shown for four mice per group. Data were analyzed using multiple Mann-Whitney tests and the Holm-Šidàk correction and represent three independent experiments. Error bars represent standard error of the mean.

(C) CD8$^{+}$ T cells purified from spleens of 8-week-old *OT-I.Nur77$^{GFP}$* or *OT-I.Drak2$^{-/-}$.Nur77$^{GFP}$* mice were cultured with antigen-presenting cells pulsed with varying concentrations of OVA-G4 or OVA$_{257–264}$ peptide for 6 h. Nur77-GFP MFI for three technical replicates is shown. Data were analyzed via two-way ANOVA with a Šidàk multiple testing correction. Error bars represent standard deviation. Data are representative of two independent experiments. $^{**}p < 0.01$, $^{***}p < 0.001$.

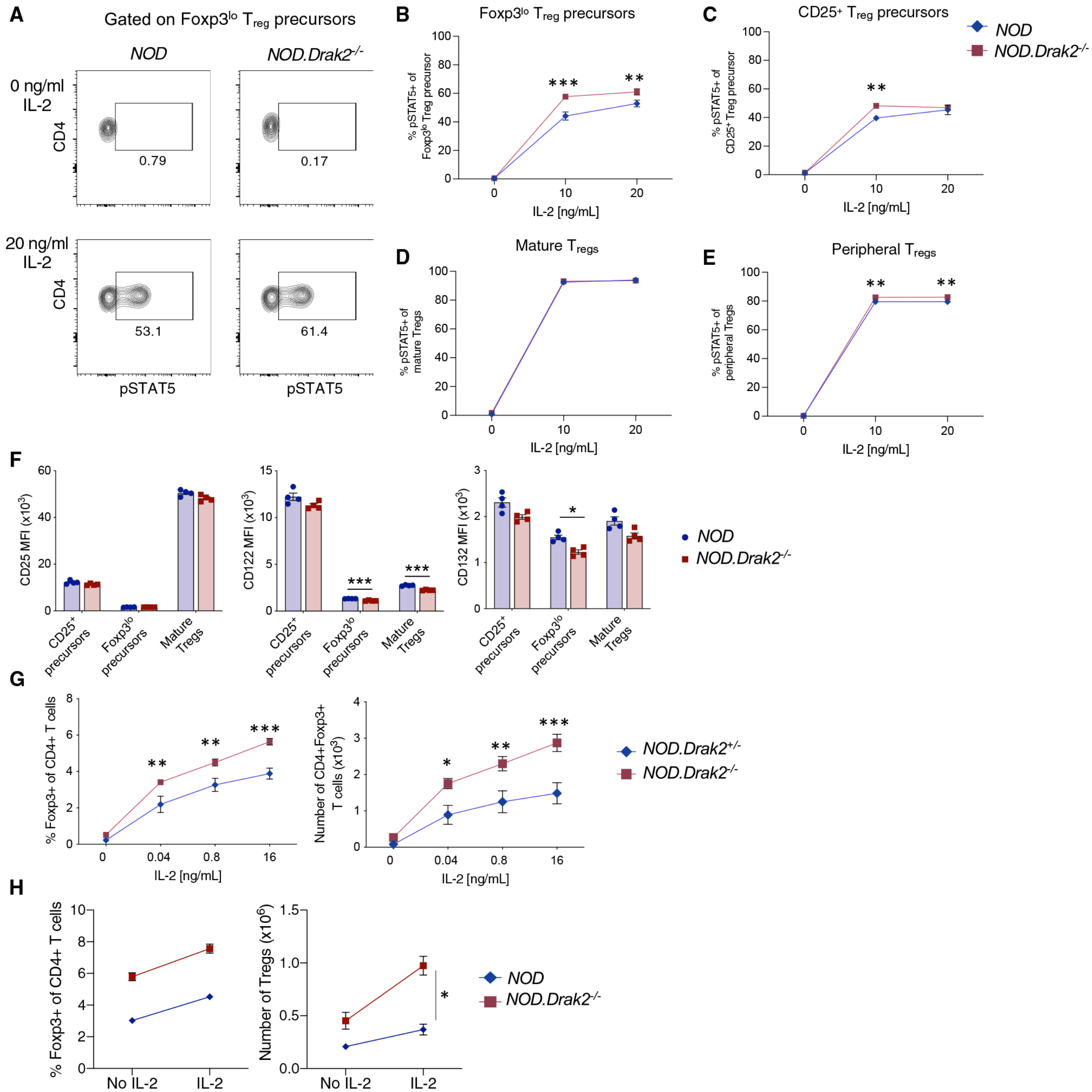


**Figure 6. DRAK2 negatively regulates IL-2 signaling in *NOD* thymocytes**

Single-cell suspensions from thymii and lymph nodes of 5-week-old *NOD* and *NOD. Drak2*$^{-/-}$ mice were stimulated with IL-2 for 15 min at 37°C. Cells were fixed and analyzed by flow cytometry to detect phosphorylated-STAT5 Y694 (pSTAT5), Foxp3, CD25, CD4, and CD8.

(A) Representative flow cytometry plots gated on CD4 SP, Foxp3$^{lo}$ $T_{reg}$ precursors (CD25$^{neg}$Foxp3$^{lo}$). The percent pSTAT5$^+$ of (B) CD4 SP Foxp3$^{lo}$ $T_{reg}$ precursors (C) CD4 SP CD25$^+$ $T_{reg}$ precursors (CD25$^+$Foxp3$^{neg}$), (D) mature thymic $T_{regs}$ (CD4$^+$CD8$^-$CD25$^+$Foxp3$^+$), and (E) lymph node $T_{regs}$ (CD4$^+$CD8$^-$Foxp3$^+$) is plotted. Data were analyzed using a two-way ANOVA with a Šidàk multiple testing correction.

(F) CD25, CD122, and CD132 MFI is shown for precursor and mature $T_{regs}$ from 4- to 6-week-old *NOD* and *NOD. Drak2*$^{-/-}$ thymii. Data were analyzed using multiple t tests with the Holm-Šidàk correction.

(G) Thymocytes from 1-day-old *NOD.Drak2*$^{+/}$ and *NOD. Drak2*$^{-/-}$ mice were incubated for 24 h with medium alone or with increasing concentrations of IL-2. The absolute number and percent Foxp3$^{+}$ cells of viable, CD4$^{+}$CD8$^{-}$ cells is shown for three to four mice per group. Data were analyzed using two-way ANOVA with a Sida ` k multiple testing correction.

(H) Four-week-old *NOD* and *NOD. Drak2*$^{-/-}$ mice were given either PBS or IL-2/anti-IL-2 complexes, i.p., daily, for 3 days. Thymii were harvested 48 h after the final injection and analyzed by flow cytometry to determine the proportion and absolute number of thymic, CD4$^{+}$CD8$^{-}$Foxp3$^{+}$ $T_{regs}$. $T_{reg}$ expansion was compared using a simple linear regression. All data represent two independent experiments. Error bars represent standard error of the mean. *$p < 0.05$, **$p < 0.01$, ***$p < 0.001$. See also Figure S5.

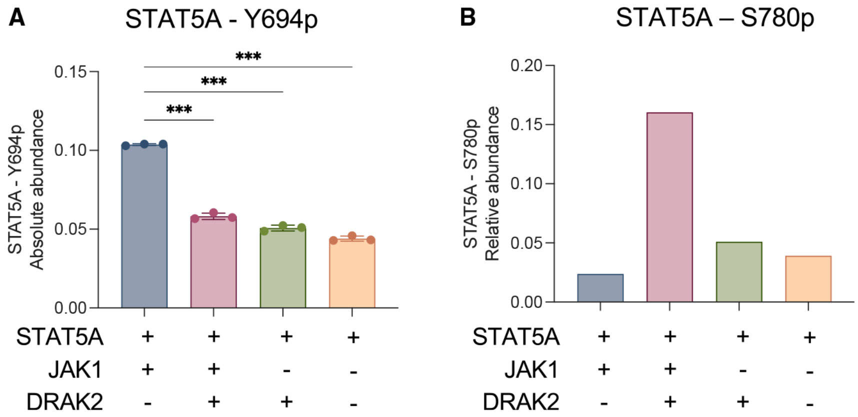


**Figure 7. DRAK2 inhibits JAK-1-mediated STAT5A phosphorylation**

Equal amounts of recombinant JAK1, STAT5A, and DRAK2 proteins were incubated in kinase reaction buffer containing ATP for 30 min. Reactions were separated by SDS-PAGE and analyzed by LC-MS/MS targeting the STAT5A Y694 residue.

(A) For quantitative analysis, stable isotope-labeled peptides containing the unmodified and phosphorylated STAT5A Y694 peptides were spiked in to serve as internal standard controls. The absolute abundance of STAT5A Y694p is calculated as the MS1 peak area across all peptide-spectrum matches (PSMs) relative to the internal standard control AQUA peptide. Error bars represent standard deviation of three technical replicates. Data were analyzed with one-way ANOVA for comparison with STAT5A phosphorylation in the presence of JAK1 only, followed by a Šidàk multiple testing correction.

(B) Abundance of STAT5A S780p relative to unmodified S780 in untargeted LC-MS/MS. Data are representative of three independent experiments. ***p < 0.001.

## KEY RESOURCES TABLE

| REAGENT or RESOURCE | SOURCE | IDENTIFIER |
|---|---|---|
| Antibodies | | |
| Anti-B220-Biotin | Biolegend | Cat# 103204; RRID: AB_312989 |
| Anti-CD4-Biotin | eBioscience | Cat# 13-0042-85; RRID: AB_466330 |
| Anti-CD4-ef450 | Invitrogen | Cat# 48-0042-82; RRID: AB_1272194 |
| Anti-CD4-BV570 | Biolegend | Cat# 100542; RRID: AB_2563051 |
| Anti-CD4-FITC | eBioscience | Cat# 11-0042-85; RRID: AB_464897 |
| Anti-CD4-BV711 | Biolegend | Cat# 100550; RRID: AB_2562099 |
| Anti-CD4-BV785 | Biolegend | Cat# 100552; RRID: AB_2563053 |
| Anti-CD4-PerCP-Cy5.5 | eBioscience | Cat# 45-0042-80; RRID: AB_906231 |
| Anti-CD4-APC | eBioscience | Cat# 17-0042-83; RRID: AB_469324 |
| Anti-CD8α-Biotin | eBioscience | Cat# 13-0081-85; RRID: AB_466347 |
| Anti-CD8α-ef450 | eBioscience | Cat# 48-0081-82; RRID: AB_1272198 |
| Anti-CD8α-V500 | BD Biosciences | Cat# 560776; RRID: AB_1937317 |
| Anti-CD8α-FITC | eBioscience | Cat# 11-0081-86; RRID: AB_464917 |
| Anti-CD8β-AF700 | Biolegend | Cat# 126618; RRID: AB_2563949 |
| Anti-CD8α-PE-Cy7 | Biolegend | Cat# 100722; RRID: AB_312761 |
| Anti-CD8α-PerCP-Cy5.5 | eBioscience | Cat# 45-0081-82; RRID: AB_1107004 |
| Anti-CD8α-APC | eBioscience | Cat# 17-0081-82; RRID: AB_469335 |
| Anti-CD8α-APC-ef780 | eBioscience | Cat# 47-0081-82; RRID: AB_1272185 |
| Anti-Cd11b-Biotin | eBioscience | Cat# 13-0112-85; RRID: AB_466360 |
| Anti-CD25-BV421 | Biolegend | Cat# 102034; RRID: AB_11203373 |
| Anti-CD25-Pacific-blue | Biolegend | Cat# 102022; RRID: AB_493643 |
| Anti-CD25-AF488 | eBioscience | Cat# 53-0252-82; RRID: AB_763470 |
| Anti-CD25-FITC | Biolegend | Cat# 102006; RRID: AB_312855 |
| Anti-CD25-BV605 | Biolegend | Cat# 102036; RRID: AB_2563059 |
| Anti-CD25-PE | BD Biosciences | Cat# 553866; RRID: AB_395101 |
| Anti-CD44-FITC | eBioscience | Cat# 11-0441-85; RRID: AB_465046 |
| Anti-CD44-BV510 | Biolegend | Cat# 103044; RRID: AB_2650923 |
| Anti-CD44-PerCP-Cy5.5 | eBioscience | Cat# 45-0441-82; RRID: AB_925746 |
| Anti-CD44-BV605 | eBioscience | Cat# 93-0441-42; RRID: AB_1257165 |
| Anti-CD44-APC | eBioscience | Cat# 17-0441-82; RRID: AB_469390 |
| Anti-CD45.1-PerCP-Cy5.5 | eBioscience | Cat# 45-0453-82; RRID:AB_1107003 |
| Anti-CD45.1-BV605 | Biolegend | Cat# 110737; RRID: AB_11204076 |
| Anti-CD45.2-BV510 | Biolegend | Cat# 109837; RRID: AB_2561393 |
| Anti-CD45.2-APC | eBioscience | Cat# 17-0454-82; RRID: AB_469400 |
| Anti-CD45RB-PE | eBioscience | Cat# 12-0455-83; RRID: AB_465682 |
| Anti-CD45RB-APC | eBioscience | Cat# 17-0455-81; RRID: AB_529535 |
| Anti-CD49b-Biotin | eBioscience | Cat# 13-5971-85; RRID: AB_466826 |
| Anti-CD62L-BV605 | Biolegend | Cat# 104438; RRID: AB_2563058 |

| REAGENT or RESOURCE | SOURCE | IDENTIFIER |
|---|---|---|
| Anti-CD62L-PE-Cy7 | Biolegend | Cat# 104418; RRID: AB_313103 |
| Anti-CD69-PE-Cy7 | eBioscience | Cat# 25-0691-82; RRID: AB_469637 |
| Anti-CD90.1-PE | eBioscience | Cat# 12-0900-81; RRID: AB_465773 |
| Anti-CD90.1-APC | eBioscience | Cat# 17-0900-82; RRID: AB_469420 |
| Anti-CD90.2-FITC | Biolegend | Cat# 105306; RRID: AB_313177 |
| Anti-CD122-BV786 | BD Biosciences | Cat# 740869; RRID: AB_2740521 |
| Anti-CD132-APC | Biolegend | Cat# 132307; RRID: AB_10643575 |
| Anti-CTLA4-PE | Biolegend | Cat# 106305; RRID: AB_313254 |
| Anti-Foxp3-ef450 | eBioscience | Cat# 48-5773-82; RRID: AB_1518812 |
| Anti-Foxp3-APC | Invitrogen | Cat# 17-5773-82; RRID: AB_469457 |
| Anti-Foxp3-PE | eBioscience | Cat# 12-5773-82; RRID: AB_465936 |
| Anti-GITR-APC | eBioscience | Cat# 17-5874-81; RRID: AB_469461 |
| Anti-Helios-PerCP-ef710 | eBioscience | Cat# 46-9883-41; RRID: AB_2573923 |
| Anti-MHCII-Biotin | eBioscience | Cat# 13-5321-85; RRID: AB_466663 |
| Anti-pSTAT5-AF488 | BD Biosciences | Cat# 612598; RRID: AB_399881 |
| Anti-pSTAT5-AF647 | Cell Signaling Technology | Cat# 9365S |
| Anti-TCRβ-BV510 | Biolegend | Cat# 109234; RRID: AB_2562350 |
| Anti-TCRβ-BV605 | Biolegend | Cat# 109241; RRID: AB_2629563 |
| Anti-IL-2 (JES6-A12) | BioXCell | Cat# BE0043; RRID: AB_1107702 |
| Chemicals, peptides, and recombinant proteins | | |
| BD Phosflow Fix Buffer I | BD Biosciences | Cat# 557870; RRID: AB_2869102 |
| BD Phosflow Perm Buffer III | BD Biosciences | Cat# 558050; RRID: AB_2869118 |
| CellTrace CFSE Cell Proliferation Kit | ThermoFisher Scientific | Cat# C34570 |
| Foxp3/Transcription Factor Staining Buffer set | eBioscience | Cat# 00-5523-00 |
| Fixable viability dye eFlour 450 | eBioscience | Cat# 65-0863-18 |
| Fixable viability dye eFlour 660 | eBioscience | Cat# 65-0864-18 |
| $OVA_{257-264}$ peptide | Hartwell Center, St. Jude | N/A |
| $OVA\text{-}G4_{257-264}$ | Hartwell Center, St. Jude | N/A |
| $OVA_{323-339}$ peptide | Hartwell Center, St. Jude | N/A |
| Recombinant mouse IL-2 | Tonbo | Cat# 21-8021 |
| Recombinant mouse IL-2 | BD Biosciences | Cat# 550069; RRID: AB_2868875 |
| Recombinant mouse IL-4 | Invitrogen | Cat# PMC0043 |
| Recombinant mouse IL-7 | Invitrogen | Cat# PMC0071 |
| Recombinant Mouse IL-15 | R&D Systems | Cat# 447-ML-010 |
| Recombinant Mouse TGF-beta | R&D Systems | Cat# 7754-BH |
| Recombinant Human JAK1 | ThermoFisher Scientific | Cat# PV4774 |
| Recombinant Human STK17B (DRAK2) | ThermoFisher Scientific | Cat# PV6328 |
| Recombinant Human STAT5α | Abcam | Cat# ab84627 |
| Synthetic STAT5α 690–700 Peptide Spike-in Sequence: AVDG(13C2)YVKPQIK | Hartwell Center, St. Jude | N/A |

| REAGENT or RESOURCE | SOURCE | IDENTIFIER |
|---|---|---|
| Synthetic phospho STAT5α 690–700 Peptide Spike-in Sequence: AVDG(13C2)Y(Phospho)VKPQIK | Hartwell Center, St. Jude | N/A |
| Critical commercial assays | | |
| RNeasy Micro Kit | Qiagen | Cat# 74004 |
| Deposited data | | |
| Microarray data | This paper | NCBI GEO: GSE210853 |
| Proteomics data | This paper | ProteomeXchange: PXD037922 |
| Experimental models: Organisms/strains | | |
| Mouse: C57BL/6J | The Jackson Laboratory | Cat# 000664; RRID: IMSR_JAX:000664 |
| Mouse: *NOD*: NOD/ShiLtJ | The Jackson Laboratory | Cat# 001976; RRID: IMSR_JAX:001976 |
| Mouse: *NOD.SCID*: NOD.Cg-Prkdc$^{scid}$/J | The Jackson Laboratory | Cat# 001303; RRID: IMSR_JAX:001303 |
| Mouse: *Nur77*$^{GFP}$: C57BL/6-Tg(Nr4a1-EGFP/cre)820Khog/J | The Jackson Laboratory | Cat# 016617; RRID: IMSR_JAX:016617 |
| Mouse: *CD45.1/1*: B6.SJL-*Ptprc*$^{a}$ *Pepc*$^{b}$/BoyJ | The Jackson Laboratory | Cat# 002014; RRID: IMSR_JAX:002014 |
| Mouse: *OT-I*: C57BL/6-Tg(TcraTcrb)1100Mjb/J | The Jackson Laboratory | Cat# 003831; RRID: IMSR_JAX:003831 |
| Mouse: *OT-I.Nur77*$^{GFP}$ | This paper | N/A |
| Mouse: *OT-II*: C57BL/6.Cg-Tg(TcraTcrb)426-6 | Kristin Hogquist | N/A |
| Mouse: *OT-II.CD45.1/2* | This paper | N/A |
| Mouse: *NOD.BDC2.5*: NOD.Cg-Tg(TcraBDC2.5,TcrbBDC2.5)1Doi/DoiJ | The Jackson Laboratory | Cat# 004460; RRID: IMSR_JAX:004460 |
| Mouse: *NOD.Thy1/1*: NOD.NON-Thy1a/1LtJ | The Jackson Laboratory | Cat# 004483; RRID: IMSR_JAX:004483 |
| Mouse: *NOD.Thy1/2* | This paper | N/A |
| Mouse: *NOD.BDC2.5.Thy1/2*: NOD.Cg-Tg(TcraBDC2.5,TcrbBDC2.5)1Doi/DoiJ: Thy1/2 | This paper | N/A |
| Mouse: *Drak2*$^{-/-}$: C57BL/6J: *Drak2*$^{-/-}$ | McGargill et al. 2004[11] | N/A |
| Mouse: *NOD.Drak2*$^{-/-}$: NOD/ShiLtJ: *Drak2*$^{-/-}$ | McGargill et al. 2008[12] | N/A |
| Mouse: *NOD.Drak2*$^{-/-}$*.SCID*: NOD.Cg-Prkdc$^{scid}$/J: *Drak2*$^{-/-}$ | This paper | N/A |
| Mouse: *Drak2*$^{-/-}$*.Nur77*$^{GFP}$: C57BL/6-Tg(Nr4a1-EGFP/cre)820Khog/J: *Drak2*$^{-/-}$ | This paper | N/A |
| Mouse: *OT-I.Drak2*$^{-/-}$: *Drak2*$^{-/-}$ | McGargill et al. 2004[11] | N/A |
| Mouse: *OT-I.Drak2*$^{-/-}$*. Nur77*$^{GFP}$: *Drak2*$^{-/-}$ | This paper | N/A |
| Mouse: *OT-II.Drak2*$^{-/-}$: *Drak2*$^{-/-}$ | McGargill et al. 2004[11] | N/A |
| Mouse:: *NOD.Drak2*$^{-/-}$*.BDC2.5*: NOD.Cg-Tg(TcraBDC2.5,TcrbBDC2.5)1Doi/DoiJ: *Drak2*$^{-/-}$ | McGargill et al. 2008[12] | N/A |
| Mouse:: *NOD.Drak2*$^{-/-}$*.BDC2.5.Thy1/2*: NOD.Cg-Tg(TcraBDC2.5,TcrbBDC2.5)1Doi/DoiJ: *Drak2*$^{-/-}$*.Thy1/2* | This paper | N/A |
| Mouse: *NOD.Drak2*$^{-/-}$*.Thy1/1*: NOD.NON-Thy1a/1LtJ: *Drak2*$^{-/-}$ | This paper | N/A |
| Software and algorithms | | |
| FlowJo | BD Biosciences | https://www.flowjo.com/ |
| Graphpad Prism | Graphpad Software | https://www.graphpad.com/scientific-software/prism// |

| REAGENT or RESOURCE | SOURCE | IDENTIFIER |
|---|---|---|
| PEAKS Studio 10.6 | Bioinformatics Solutions Inc. | https://www.bioinfor.com/peaks-studio/ |
| ProteoWizard 3.0 | Chambers et al. 2012[52] | https://proteowizard.sourceforge.io/ |
| Skyline | Pino et al. 2020[53] | https://skyline.ms/wiki/home/software/Skyline/page.view?name=default |
| R | The R Core Team | https://www.r-project.org/ |
| R package "ggplot2" | Wikham et al. 2016[54] | https://cran.r-project.org/web/packages/ggplot2/index.html |
| R package "limma" | Ritchie et al. 2015[55] | https://bioconductor.org/packages/release/bioc/html/limma.html |
| R package "oligo" | Carvalho and Irizarry,.2010[56] | https://bioconductor.org/packages/release/bioc/html/oligo.html |
| Other | | |
| Anti-CD45R/B220 Microbeads | Miltenyi Biotec | Cat# 130-049-501 |
| Dynabeads Mouse T-Activator CD3/CD28 | Invitrogen | Cat# 114-52D |
| Streptavidin Microbeads | Miltenyi Biotec | Cat# 130-048-101 |